Fermilab-Pub-13-091-PPD

B-PHYSICS RESULTS FROM TEVATRON

Guennadi Borissov *

Department of Physics, Lancaster University,
Lancaster, LA1 4YB, United Kingdom

g.borissov@lancaster.ac.uk

4 January 2013

Abstract

This review summarizes the most important results in B physics obtained at the Tevatron. They include the discovery of the new B hadrons, the measurement of their masses and lifetimes, the measurement of the oscillation frequency of B_s^0 meson, the search for its rare decay $B_s^0 \to \mu^+\mu^-$, and the study of the CP asymmetry in decays and mixing of B mesons.

PACS numbers: 14.65.Fy, 14.40.Nd, 14.20.Mr, 13.20.He, 13.25.Hw

1 Introduction

The experiments CDF and DØ collected more than 10 fb^{-1} of $p\bar{p}$ collisions in RunII of the Tevatron collider at Fermilab from 2002 to 2011 at a center of mass energy $\sqrt{s} = 1.96$ TeV. It was the world highest energy during almost the entire period of data taking, which allowed the experiments to search for new phenomena at the energy frontier of the particle physics. Namely this search at the highest possible collision energy and in particular hunting for new heavy particles was the main goal of both experiments. They were designed accordingly as the multipurpose detectors capable to detect and study the processes with the center of mass energy of the order of 1 TeV.

However, both experiments in the same time actively pursued the study of B hadrons. This direction may look unusual and unexpected for the Tevatron, as the high energy of $p\bar{p}$ collisions is not needed, while the high multiplicity and the overwhelming background coming from light quark and gluon interactions are clearly obstructive for this kind of research. What is required, on the contrary, is a dedicated experimental facility with such special features as sophisticated trigger on B-hadron production, exclusive reconstruction of all B-hadron decay

*To be published in International Journal of Modern Physics A

products, both charged and neutral, precise measurement of their trajectories and identification of their type. These requirements were only partially satisfied for the CDF and DØ detectors. On the contrary, the specialised experiments at B factories, such as BaBar and Belle, were operational at the same time as the Tevatron experiments, possessed all these qualities and ran in a much cleaner environment of e^+e^- collisions. And it would seem hopeless to compete with them, so that any study at hadron collider would be doomed to be the second class physics.

Nevertheless, the B-physics research at hadron collider does offer several unique possibilities, which are not available anywhere else. The cross section of $b\bar{b}$ production at the Tevatron is significantly higher than that at the e^+e^- colliders. Therefore, an enormous statistics of events containing B hadrons is accessible. Of course, not all B events were recorded by the experiments, but the large number of produced B hadrons allowed to build highly selective triggers on interesting events and study very rare decays of B hadrons, such as $B^0, B_s^0 \to \mu^+\mu^-$, or statistically limited processes, like the dimuon charge asymmetry. The second important feature is the production of all species of B hadrons in $p\bar{p}$ collisions, while only $B^\pm$ and B^0 mesons can be studied at the B factories where B hadrons are mainly created in the decays of $\Upsilon(4S)$ meson. This possibility allowed the experiments at the Tevatron to perform many unique measurements, such as the oscillation of B_s^0 meson, the lifetime and the mass of $B_c^\pm$ mesons, the discovery of baryons containing b quark. The third advantage of the Tevatron experiments is a large momentum boost of B hadrons. This boost considerably increases their mean decay length in the laboratory frame. At B factories, on the contrary, B hadrons are produced at the mass threshold and their momentum in the laboratory frame is relatively small. Due to this boost, a more precise measurement of the B-hadron proper lifetime is possible at the Tevatron. This advantage becomes essential, e.g., for the study of the time evolution of the B_s^0 system.

It is quite difficult to exploit these advantages to a full extent. The cross section of background processes in $p\bar{p}$ collisions at $\sqrt{s} = 1.96$ TeV is ~ 800 times larger than that of the $b\bar{b}$ production. The only possibility to suppress this background is to analyse a limited number of special decay modes of B hadrons, like the decays containing $J/\psi \to \mu^+\mu^-$ meson, or simple hadronic decay modes, such as $B_s \to D_s\pi$. In each event many background particles from the $p\bar{p}$ interactions accompany the B-hadron decay products. In addition, the Tevatron experiments in their quest for new physics ran at the highest possible accelerator luminosity, so that each recorded event, beside the $b\bar{b}$ production, contains in average three background pile-up interactions. As a result, an event at hadron collider looks very complicated. The mean multiplicity of reconstructed charged particles in a typical recorded event is about 80, with a very long tail extending above 300 tracks. Therefore, selecting the charged B hadron decay products among all background tracks results in a large combinatorial background which should be suppressed by additional requirements. And due to the presence of a large number of background particles it is almost impossible to select neu-

tral particles from B-hadron decay,[1] since there is no any handle to associate correctly the clusters in the calorimeters with decaying B hadron.

In addition to these difficulties, the Tevatron detectors were not especially built for the B-physics study, and, e.g., their particle identification was insufficient for many tasks. The B-physics research program competed with other high profile tasks, like the search for the Higgs boson or the study of top quark. Therefore, the material and human resources available for B-physics studies were limited and these studies were performed by a relatively small number of dedicated scientists.

All these problems are very serious and disadvantageous, and nevertheless the B-physics research at the Tevatron was proven to be very successful. One of the important accomplishments of the CDF and DØ experiments was namely this convincing demonstration that, in spite of all obstacles, performing the B-physics research at hadronic collider is a very rewarding experience producing unique, world best and valuable results. This success was achieved, among other means, by a clear definition of research goals, by fully exploiting the advantages provided by the hadron colliders and detectors, and by pursuing a relatively small number of high profile measurements which can compete with, or simply cannot be performed at the B factories.

The aim of this review is to summarize the most important, from the author's point of view, B-physics results obtained by the CDF and DØ collaborations. The Tevatron achievements in B physics provide an excellent starting point for the LHC experiments at CERN, which continue and extend many studies started at Fermilab, and which need to overcome similar or even greater problems while performing the B-physics studies. Therefore, the experience learned at the Tevatron can be useful for the next generation of experiments at hadron colliders, and one of the aims of this review is to share it. Due to the size limitation, this review is not expected to be complete and exhaustive, and many excellent results from the Tevatron will stay beyond the scope of this paper.

After a brief discussion of the CDF and DØ detectors in Section 2, with the emphasis on the parts and features essential for the B-physics studies, I will review the discovery of the new B hadrons in Section 3 and the measurement of the B-hadron lifetimes in Section 4. The breakthrough measurement of the oscillation frequency of the B_s^0 meson is presented in Section 5. The study of the decays of B mesons, including the search for the rare decays providing strong constraint on the new physics contribution is given in Section 6. Finally, the study of the CP asymmetry in B-meson decays and mixing is discussed in Section 7.

[1] A rare exception is the reconstruction of K_S meson and Λ baryon using their decays $K_S \to \pi^+\pi^-$ and $\Lambda \to p\pi^-$, and of the photon using its conversion $\gamma \to e^+e^-$ in the detector material.

2 Detectors

The CDF and DØ experiments are the general purpose collider detectors constructed to maximally exploit the possibilities provided by the $p\bar{p}$ collisions at $\sqrt{s} = 1.96$ TeV and to operate at the instantaneous luminosity up to 5×10^{32} cm^{-2} s^{-1}. Although the main emphasis in their design is made on the detection of events with the highest possible invariant mass, they also contain the specific elements necessary to endeavour the B-physics research.

The tracking system of the CDF detector[1] includes the solenoidal magnet producing a uniform magnetic field of 1.4 T, the inner tracking volume containing the silicon microstrip detectors up to a radius of 28 cm from the beamline[2], and the outer tracking volume instrumented with an open-cell drift chamber[3] (COT) up to the radius of 137 cm. The first single-sided layer of the silicon detector[4] is mounted directly on the beam-pipe at the radius of 1.5 cm. The tracking systems reconstructs the trajectory and momentum of the charged particles up to the pseudorapidity[2] $|\eta| < 2$. The resolution of the track impact parameter[3] is about 40 μm. This resolution includes an uncertainty of the interaction point in the transverse plane, which is about 30 μm. The momentum resolution of the tracking system is $\sigma(p_T)/p_T^2 \simeq 1.7 \times 10^{-3}$ GeV^{-1}, where p_T is the component of the particle momentum transversal to the beam direction.

The muon identification system[5, 6] is located after the magnet and the calorimeters, which serve as a shield to suppress the penetration of all charged and neutral particles except the muons. It includes the drift chambers, which detect muons with $p_T > 1.4$ GeV within $|\eta| < 0.6$, and additional chambers and scintillators, which cover $0.6 < |\eta| < 1.0$ for muons with $p_T > 2.0$ GeV.

An important component of the CDF detector essential for the B-physics measurements is the special trigger selecting events with displaced tracks. It is a three-level system. At the first level[7] the COT hits are grouped into tracks in the transverse plane. At the second level[8], the silicon hits are added to the tracks found at the first level. These hits improve the resolution of the track impact parameter, which is measured in real time. Finally, the displaced vertex trigger[9] requires two charged particles with $p_T > 2$ GeV, and with impact parameters in the range $0.12 - 1$ mm. This trigger configuration is the basis for many CDF measurements with fully hadronic B decays. Its other trigger configurations select the events with one or two muons.

The central tracking system of the DØ detector[10] comprises a silicon microstrip tracker and a central fiber tracker, both located within a 1.9 T superconducting solenoidal magnet. The outer radius of the tracking system is 52 cm. The tracking system reconstructs tracks with $|\eta| < 2.2$. The closest to the beam layer of the silicon detector[12, 13] is located at the radius 1.7 cm. The impact parameter precision of high momentum tracks is ~ 18 μm. The momentum resolution provided by the tracking system is $\sigma(p_T)/p_T^2 \simeq 3.0 \times 10^{-3}$ GeV^{-1} for

[2] The pseudorapidity is defined as $\eta = -\ln(\tan(\theta/2))$, where θ is the polar angle of charged track relative to the direction of the proton beam.

[3] The impact parameter is defined as the distance of closest approach of the charged particle to the $p\bar{p}$ interaction point in the plane transverse to the beam direction.

tracks with $p_T > 5$ GeV.

The muon system[11] is located beyond the calorimeters that surround the central tracking system, and consists of a layer of tracking detectors and scintillation trigger counters before 1.8 T iron toroids, followed by two similar layers after the toroids. It is able to identify the muons with $|\eta| < 2.0$. The toroidal magnets allow an independent measurement of the muon momentum, which helps to improve the quality of identified muons.

The trigger system of the DØ detector does not provide a possibility to collect events with displaced tracks, although its muon and di-muon triggers are very efficient and robust. Therefore the focus of the B-physics measurements in DØ experiment is shifted towards the semileptonic B decays and decays with $J/\psi \to \mu^+\mu^-$ in the final state.

The polarities of the toroidal and solenoidal magnetic fields of the DØ detector are regularly reversed. This reversal helps to significantly reduce the systematic uncertainties of the measurements sensitive to the differences in the reconstruction efficiency between the positive and negative particles, like the measurements of the CP violating charge asymmetries.

Thus, both experiments have sufficient and powerful tools to fulfil their B-physics research program. They also contain several special features which make them different and complementary. The CDF detector has a larger tracking volume. Therefore its charged particle momentum resolution is superior to that of the DØ detector. It also can select the hadronic B decays. The DØ detector includes a sophisticated muon identification system with local measurement of muon momentum. It extends up to $|\eta < 2.0|$ and provides a clean selection of muons with strong background suppression. The reversal of magnet polarities allows it to perform several measurements of the charge asymmetry in the semileptonic B decays which are at the world best level.

3 Discovery of New Particles containing b quark

The search for new particles is always a very exciting task. Historically, namely such a search helped to establish, e.g., the quark model or the Standard Model (SM) of electro-weak interactions as true theories. The quark model describes the observed hadrons as the bound states of quarks and anti-quarks. It predicts in particular the spectrum of particles containing b quark. Various theoretical techniques based on the quark model are developed to compute the properties of these particles. Comparison of these predictions with the experimental observations helps to improve and rectify these techniques and develop new more powerful methods. Therefore, discovery of new particles containing b quarks constitutes an important part of B physics. An observation of each new object attracts a lot of attention in particle physics community, and each such observation provides a new confirmation of the validity and strength of the quark model. Since all types of B hadrons can be produced at hadron colliders with relatively high production rate, it is an ideal place for this kind of research. The discovery of several such objects by the experiments at the Tevatron is described

in this section.

3.1 Mass of B_s^0 meson and Λ_b^0 baryon

Although the B_s^0 meson and Λ_b^0 baryon were first observed at LEP [14], their mass was first precisely measured by the CDF collaboration. The CDF measured simultaneously the masses of B^+, B^0, B_s^0 mesons and Λ_b^0 baryon [15]. The comparison of the B^+ and B^0 mass with the results obtained at the e^+e^- collider by the CLEO collaboration [16] provides an excellent cross-check of the measurement technique and gives a confidence in the values of the B_s^0 and Λ_b^0 mass, which was known with a very poor precision at that time. The obtained results are:

$$m(B^+) = 5279.10 \pm 0.41(\text{stat}) \pm 0.36(\text{syst}) \text{ MeV}, \quad (1)$$

$$m(B^0) = 5279.63 \pm 0.53(\text{stat}) \pm 0.33(\text{syst}) \text{ MeV}, \quad (2)$$

$$m(B_s^0) = 5366.01 \pm 0.73(\text{stat}) \pm 0.33(\text{syst}) \text{ MeV}, \quad (3)$$

$$m(\Lambda_b^0) = 5619.7 \pm 1.2 \text{ (stat)} \pm 1.2 \text{ (syst) MeV}. \quad (4)$$

The achieved precision of the B^+ and B^0 mass is compatible or even better than the CLEO values, while the precision of the B_s^0 and Λ_b^0 mass is improved by more than 10 times compared to the previous LEP measurements. Recently, the LHCb collaboration obtained the most precise values of the B-hadron masses [17], which agree well with the CDF results.

3.2 $B_c^\pm$ meson

The B_c^- mesons contains b quark and c anti-quark. A relatively heavy mass of these quarks simplifies the theoretical calculations of the $B_c^\pm$ properties. For lattice QCD model, the $B_c^\pm$ is called a "gold-plated" hadron [18]. However, various theoretical models predict different mass ranges for this particle with large uncertainties. Non-relativistic quark models [19, 20, 21] predict the $B_c^\pm$ mass in the range 6247 – 6286 MeV. The lattice QCD calculations[22] provide a slightly different mass value $M(B_c^\pm) = 6304 \pm 12^{+18}_{-0}$ MeV. Therefore, a precise measurement of the $B_c^\pm$ mass is essential for verifying these calculations and improving the computational techniques.

The first precise measurement of the $B_c^\pm$ mass was done in the decay mode $B_c^\pm \to J/\psi\pi^\pm$, with $J/\psi \to \mu^+\mu^-$, by the CDF collaboration [23] using the data corresponding to an integrated luminosity of 2.4 fb^{-1} . It is the easiest decay mode to separate the $B_c^\pm$ production from background because of the clean muon identification and the pure $J/\psi \to \mu^+\mu^-$ decay selection. A set of cuts to select the signal was developed and tested using the decay $B^\pm \to J/\psi K^\pm$, which has a similar final state topology with the only difference that the $\pi^\pm$ meson in $B_c^\pm$ decay is replaced by the $K^\pm$ meson. Since the lifetime of $B_c^\pm$ meson is much shorter than the lifetime of $B^\pm$ meson, only the $B^\pm \to J/\psi K^\pm$ candidates with proper decay length $80 < ct < 300$ μm were used to test the selection criteria. The mass distribution of the selected $B_c^\pm \to J/\psi\pi^\pm$ candidates is shown in Fig.

1. An excess of $J/\psi\pi^{\pm}$ events with the invariant mass around 6280 MeV is clearly seen. The unbinned fit over the mass range 6150 - 6500 MeV gives a $B_c^{\pm}$ signal of 108 ± 15 candidates with a mass of

$$m(B_c^{\pm}) = 6275.6 \pm 2.9(\text{stat}) \pm 2.5(\text{syst}) \text{ MeV}. \quad (5)$$

The statistical significance of this observation corresponds to 8 standard deviations.

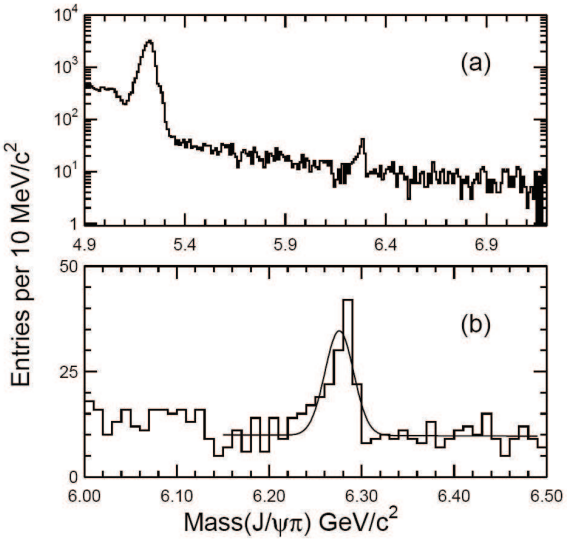

Figure 1: (a). The invariant mass distribution of $J/\psi K^{\pm}$ combinations from Ref. [23]. (b) Identical to (a), but in a narrower mass range. The projection of the fit to the data is indicated by the curve overlaid on (b).

The DØ collaboration performed a similar analysis of the $J/\psi\pi^{\pm}$ final state [24]. They used the integrated luminosity 1.3^{-1} fb. The resulting invariant mass distribution of the selected $J/\psi\pi^{\pm}$ combinations is shown in Fig. 2. The unbinned fit of selected events gives 54 ± 12 events and the $B_c^{\pm}$ mass

$$m(B_c^{\pm}) = 6300 \pm 14(\text{stat}) \pm 5(\text{syst}) \text{ MeV}. \quad (6)$$

The statistical significance of the observed $B_c^{\pm}$ signal exceeds 5 standard deviations above the background level.

Comparing the results of the two experiments, it is clearly seen that the mass resolution in the CDF experiments is much better, which is reflected in a smaller uncertainty of the measured $B_c^{\pm}$ mass and smaller background level for the CDF measurement. This difference is mainly caused by ~ 2.5 times larger tracking volume of the CDF detector, which gives a significant gain in the momentum resolution of the charged particles. Nevertheless, the result of

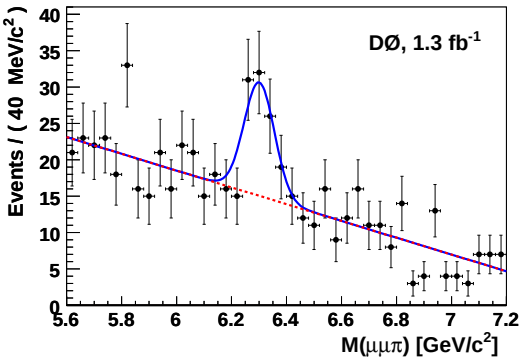

Figure 2: The $J/\psi\pi^{\pm}$ invariant mass distribution of $B_c^{\pm}$ candidates from Ref. [24]. A projection of the unbinned maximum likelihood fit to the distribution is shown overlaid.

DØ experiment provides an important confirmation of the CDF observation. The two measurements of the $B_c^{\pm}$ mass agree within 2 standard deviations, so that the existence of the $B_c^{\pm}$ is firmly established. The recent result of the LHCb experiment [25], which obtains

$$m(B_c^{\pm}) = 6273.7 \pm 1.3(\text{stat}) \pm 1.6(\text{syst})\text{MeV}, \tag{7}$$

confirms these two observations.

3.3 $\Sigma_b^{\pm}$ and $\Sigma_b^{*\pm}$ baryons

The quark model predicts the existence of many baryons containing b quark, but only the Λ_b baryon with quark content (bdu) was observed before the start of the experiments at the Tevatron. The search for other B baryons at CDF and DØ experiments was very fruitful, as essentially all baryons with one b quark, except Σ_b^0 baryon with quark content (bdu), were discovered by them. The theory also predicts the mass of all these objects and other properties which can be tested experimentally, although different models give slightly different values. Therefore, an observation of these objects provides direct comparison with theory, which is essential for verifying theoretical models and helping to improve them.

The quark content of $\Sigma_b^{(*)+}$ baryon[4] is (buu) and the quark content of $\Sigma_b^{(*)-}$ baryon is (bdd). Thus, they are different particles with different mass. In the heavy quark effective theory (HQET)[26], describing these objects, a heavy b quark is considered as static and surrounded by a diquark system of two light

[4]The notation $\Sigma_b^{(*)\pm}$ refers to the states $\Sigma_b^{\pm}$ and $\Sigma_b^{*\pm}$.

quarks. This diquark system has isospin $I = 1$ and $J^P = 1^+$, so that the lightest quark systems (buu) and (bdd) can have the quantum numbers $J^P = \frac{1}{2}^+$ $(\Sigma_b^{\pm})$ and $J^P = \frac{3}{2}^+$ $(\Sigma_b^{*\pm})$. An extensive list of theoretical papers, predicting the masses of $\Sigma_b^{(*)\pm}$ baryons can be found in Ref. [27], here we give just some of them.[28, 29, 30, 31, 32, 33, 34, 35] Based on these works, the mass difference between $\Sigma_b^{(*)\pm}$ and Λ_b baryons is expected to be $m(\Sigma_b) - m(\Lambda_b) \sim 180 - 210$ MeV; therefore, the main decay mode of $\Sigma_b^{(*)\pm}$ should be $\Sigma_b^{(*)\pm} \to \Lambda_b \pi^{\pm}$.

The observation of these particles were first reported by the CDF collaboration in Ref. [36], and the following paper[27] gives an improved measurement of their mass using the integrated luminosity 6 fb^{-1}. The $\Sigma_b^{(*)\pm}$ baryons were searched for in the decay $\Sigma_b^{(*)\pm} \to \Lambda_b \pi^{\pm}$, with $\Lambda_b \to \Lambda_c^+ \pi^-$ and $\Lambda_c^+ \to pK^-\pi^+$. The decays were selected with the displaced two-track trigger, which allowed the CDF experiment to collect the events with hadronic decays of heavy hadrons. There was not such a possibility in the DØ detector and it does not have any result on the studies involving the hadronic decays of B hadrons.

Using the sample of approximately 16300 reconstructed Λ_b decays, the CDF collaboration built the mass difference

$$Q = m(\Lambda_b \pi) - m(\lambda_b) - m(\pi), \tag{8}$$

which is shown in Fig. 3. The signals of both $\Sigma_b^{\pm}$ and $\Sigma_b^{*\pm}$ are clearly seen. The parameters of all four baryons obtained from the fit of these distributions are given in Table 1.

Table 1: Parameters of $\Sigma_b^{(*)\pm}$ baryons from Ref. [27]. The first uncertainty is statistical and the second is systematic.

State	Q value (MeV)	Mass m (MeV)	Natural width Γ (MeV)
Σ_b^-	$56.2\ ^{+0.6}_{-0.5}\ ^{+0.1}_{-0.4}$	$5815.5^{+0.6}_{-0.5} \pm 1.7$	$4.9^{+3.1}_{-2.1} \pm 1.1$
Σ_b^{*-}	$75.8 \pm 0.6^{+0.1}_{-0.6}$	$5835.1 \pm 0.6^{+1.7}_{-1.8}$	$7.5\ ^{+2.2}_{-1.8}\ ^{+0.9}_{-1.4}$
Σ_b^+	$52.1\ ^{+0.9}_{-0.8}\ ^{+0.1}_{-0.4}$	$5811.3^{+0.9}_{-0.8} \pm 1.7$	$9.7\ ^{+3.8}_{-2.8}\ ^{+1.2}_{-1.1}$
Σ_b^{*+}	$72.8 \pm 0.7^{+0.1}_{-0.6}$	$5832.1 \pm 0.7^{+1.7}_{-1.8}$	$11.5\ ^{+2.7}_{-2.2}\ ^{+1.0}_{-1.5}$

In addition, the CDF collaboration measured the isospin mass splitting between the positive and negative Σ_b baryons:

$$m(\Sigma_b^+) - m(\Sigma_b^-) = 4.2^{+1.1}_{-1.0} \pm 0.1 \text{ MeV}, \tag{9}$$

$$m(\Sigma_b^{*+}) - m(\Sigma_b^{*-}) = 3.0^{+1.0}_{-0.9} \pm 0.1 \text{ MeV}. \tag{10}$$

Thus, the $\Sigma_b^{(*)-}$ baryons are heavier than the $\Sigma_b^{(*)+}$ baryons, which is similar to the pattern observed in all other isospin multiplets. It can be explained by the

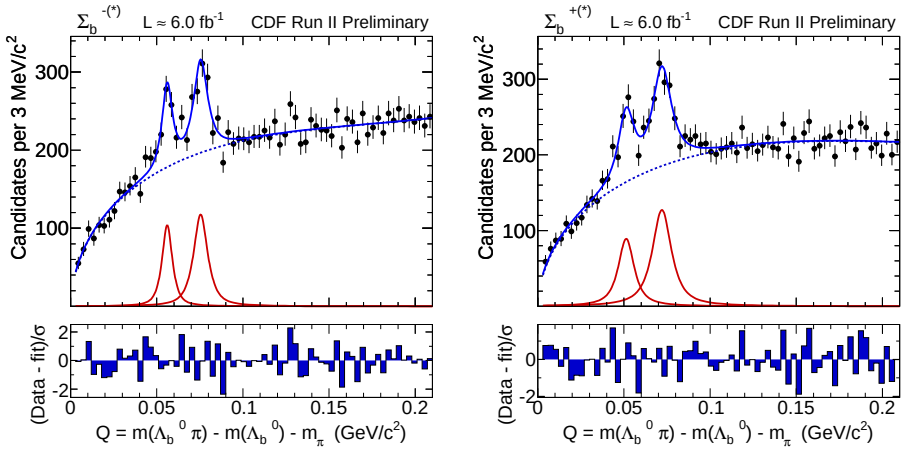

Figure 3: The left (right) plot shows the Q-value spectrum for Σ_b^- (Σ_b^+) candidates from Ref. [27] with the projection of the corresponding unbinned likelihood fit superimposed. The Q value is defined in Eq. (8). The pull distribution of each fit is shown in the bottom of the corresponding plot.

larger mass of the d quark with respect to the u quark. The electromagnetic contribution due to electrostatic Coulomb forces between quarks, which is larger in $\Sigma_b^{(*)-}$ baryons than in $\Sigma_b^{(*)+}$ baryons, can also contribute in the observed mass splitting.

3.4 $\Xi_b^\pm$ baryon

The Ξ_b^- baryon with the quark content (bds) contains the down-type quarks from all three families. Since it contains the s quark, it decays weakly and has a relatively long lifetime with its decay vertex separated from the primary interaction. It was first discovered by DØ collaboration[37] and confirmed by the CDF collaboration[38] soon after that. It was observed in the decay mode $\Xi_b^- \to J/\psi\Xi^-$ with $J/\psi \to \mu^+\mu^-$, $\Xi^- \to \Lambda\pi^-$, and $\Lambda \to p\pi^-$. Reconstruction of this decay chain is quite difficult because it contains three separate decay vertices as can be seen in Fig. 4.

Both collaborations developed sophisticated selections to suppress a background and obtain a clean signal. In particular, they utilize the relatively long lifetime of $\Xi_b^\pm$ baryon and a distinctive separation of its decay vertex from the primary interaction point. As a result, the suppression of background for this final state is strong, and a clean $\Xi_b^\pm$ signal is obtained. The left plot in Fig. 5 shows the $J/\psi\Xi^\pm$ mass distribution obtained by the DØ collaboration after all selection criteria applied, while the right plot shows the similar mass distribu-

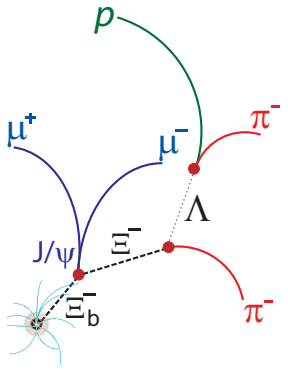

Figure 4: Schematic of the $\Xi_b^- \to J/\psi\Xi^- \to J/\psi\Lambda\pi^- \to (\mu^+\mu^-)(p\pi^-)\pi^-$ decay topology taken from Ref. [37]. The Λ and Ξ^- baryons have decay lengths of the order of cm; the Ξ_b^- baryon has a decay length of the order of mm.

tion obtained by the CDF collaboration. In both cases, a clean and statistically significant signal of the $\Xi_b^\pm$ production is observed.

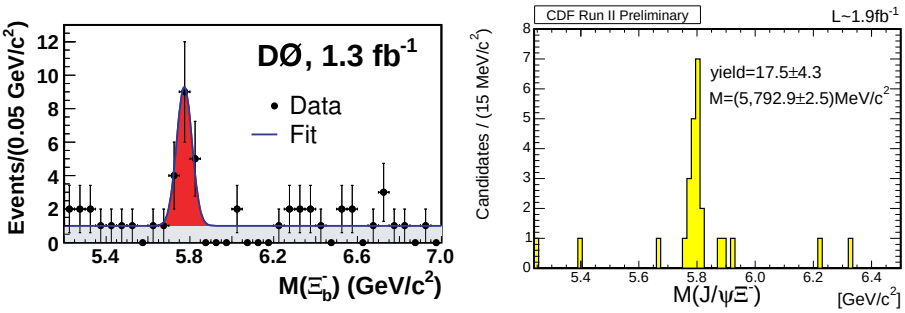

Figure 5: The left (right) plot shows the $J/\psi\Xi^\pm$ invariant mass distribution obtained by the DØ (CDF) collaboration, and taken from Ref. [37] ([38]), respectively.

The measured mass of the $\Xi_b^\pm$ baryon is found to be

$$m(\Xi_b^\pm) = 5774 \pm 11(\text{stat}) \pm 17(\text{syst}) \text{ MeV (DØ Collab.)}, \quad (11)$$
$$m(\Xi_b^\pm) = 5792.9 \pm 2.5(\text{stat}) \pm 1.7(\text{syst}) \text{ MeV (CDF Collab.)}. \quad (12)$$

Again, a better precision of the CDF measurement is mainly due to a better precision of the tracking system of the CDF detector. In the most recent

measurement[39] the CDF collaboration reports a statistically consistent value of the mass with the improved systematic uncertainty

$$m(\Xi_b^{\pm}) = 5790.9 \pm 2.6(\text{stat}) \pm 0.8(\text{syst}) \text{ MeV}. \quad (13)$$

The obtained $\Xi_b^{\pm}$ mass is in a qualitatively good agreement with the theoretical predictions[28, 29, 30, 31, 32, 33, 34].

3.5 Ξ_b^0 baryon

The Ξ_b^0 baryon is the isospin partner of the Ξ_b^- baryon and has the quark content (usb). Contrary to Ξ_b^- baryon, there is no Ξ_b^0 decay mode containing $J/\psi \to \mu^+\mu^-$ and charged particles, therefore it can not be studied in the DØ experiment. It is observed by the CDF collaboration[40] in the decay mode $\Xi_b^0 \to \Xi_c^+\pi^-$, where $\Xi_c^+ \to \Xi^-\pi^+\pi^+$, $\Xi^- \to \Lambda\pi^-$, and $\Lambda \to p\pi^-$. The data sample used for this observation corresponds to an integrated luminosity of 4.2 fb^{-1} and is collected using the displaced two-track trigger. In parallel, the same analysis searched for the decay $\Xi_b^- \to \Xi_c^0\pi^-$, with $\Xi_c^0 \to \Xi^-\pi^+$. It was selected using similar criteria and the same trigger. Since the Ξ_b^- baryon was established by the time of this study, this decay provides an excellent cross check of the full analysis chain applied in the search for the new particle.

The obtained distributions of the $\Xi_c^+\pi^-$ and $\Xi_c^+\pi^-\pi^-$ invariant mass are shown in Fig. 6. The signals of both $\Xi_b^- \to \Xi_c^0\pi^-$ and $\Xi_b^0 \to \Xi_c^+\pi^-$ decays are clearly seen. In total, $25.3^{+5.6}_{-5.4}$ candidates of the $\Xi_b^0 \to \Xi_c^+\pi^-$ decay are observed with the significance greated than 6 standard deviations. The measured mass of Ξ_b^0 baryon is found to be

$$m(\Xi_b^0) = 5787.8 \pm 5.0(\text{stat}) \pm 1.3(\text{syst}) \text{ MeV}. \quad (14)$$

In addition, the first observation of the $\Xi_b^- \to \Xi_c^0\pi^-$ decay is reported with $25.8^{+5.5}_{-5.2}$ candidates selected.

3.6 $\Omega_b^{\pm}$ baryon

The Ω_b^- baryon contains (bss) quarks. It was observed by the DØ[41] and CDF [39] collaborations in the decay mode $\Omega_b^- \to J/\psi\Omega^-$ with $J/\psi \to \mu^+\mu^-$, $\Omega^- \to \Lambda K^-$, and $\Lambda \to p\pi^-$. This decay mode is similar to the decay mode used for the $\Xi_b^{\pm}$ discovery with $\Xi^- \to \Lambda\pi^-$ replaced by the $\Omega^- \to \Lambda K^-$ decay, i.e., the same group of charged particles and the same vertex topology is selected as for the search for $\Xi_b^{\pm}$, with one of the particles assigned the mass of kaon instead of pion.

The results of both experiments are shown in Fig. 7. The measured mass of the $\Omega_b^{\pm}$ baryon is found to be

$$m(\Omega_b^{\pm}) = 6165 \pm 10(\text{stat}) \pm 15(\text{syst}) \text{ MeV (DØ Collab.)}, \quad (15)$$

$$m(\Omega_b^{\pm}) = 6054.4 \pm 6.8(\text{stat}) \pm 0.9(\text{syst}) \text{ MeV (CDF Collab.)}. \quad (16)$$

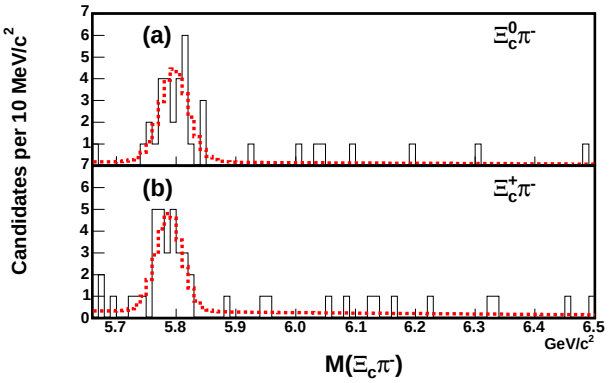

Figure 6: (a) The $\Xi_b^- \to \Xi_c^0\pi^-$ and (b) the $\Xi_b^0 \to \Xi_c^+\pi^-$ mass distributions from Ref. [40]. A projection of the likelihood fit is overlaid as a dashed line.

There is a clear disagreement between these two measurements with the difference between them $111 \pm 12(\text{stat}) \pm 14(\text{syst})$ MeV. Thus, a complementary measurement by an indpendent experiment is required to resolve this controversy. Nevertheless, the statistical significance of the observed signal is sufficient to claim the observation of this baryon by both the DØ and CDF experiments.

3.7 Excited B mesons

In addition to the ground state B mesons with spin-parity $J^P = 0^-$ ($B^\pm$, B^0, B_s^0, $B_c^\pm$) and B^* mesons ($J^P = 1^-$) with internal orbital momentum $L = 0$, the quark model predicts a rich spectrum of excited B mesons with higher values of L. In particular, for $L = 1$, there should be the broad states B_0^* ($J^P = 0^+$) and B_1^* ($J^P = 1^+$), and the narrow states B_1 ($J^P = 1^+$) and B_2^* ($J^P = 2^+$). [42, 43, 44, 45, 46, 47, 48, 49, 50, 51] The broad states decay through an S wave and therefore have widths of a few hundred MeV. Such states are difficult to distinguish in the invariant mass distribution from the combinatorial background. The narrow states decay through a D wave and therefore should have widths of around 10 MeV. The masses, widths and the relative branching fractions of these states are predicted with good precision by the theoretical models and can be compared with the experimental results.

Both collaborations preformed the measurements of the neutral narrow excited B mesons. The direct decay $B_1^0 \to B^+\pi^-$ is forbidden by conservation of parity and angular momentum. Therefore, this meson was searched for in the decay mode $B_1^0 \to B^{*+}\pi^-$ with $B^{*+} \to B^+\gamma$. On the contrary, both decays $B_2^{*0} \to B^{*+}\pi^-$ and $B_2^{*0} \to B^+\pi$ are allowed, and the corresponding branch-

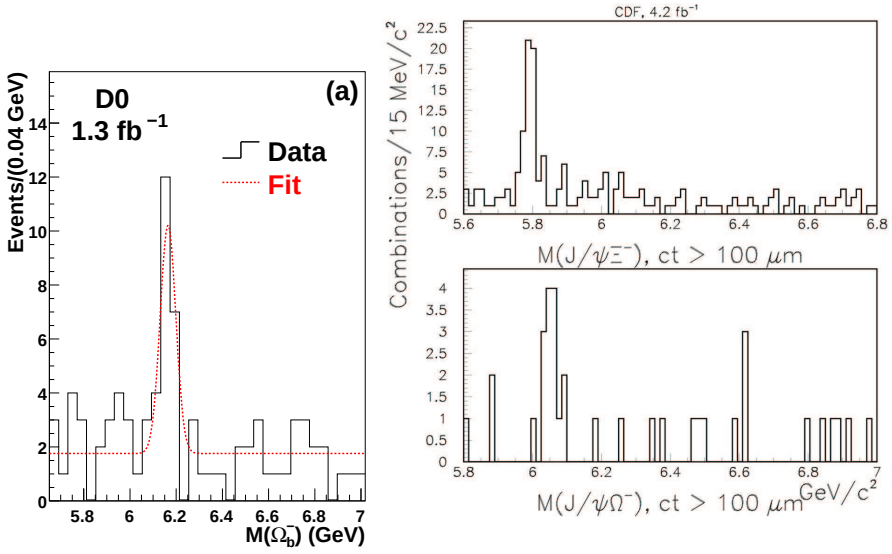

Figure 7: The left (right) plot shows the $J/\psi\Omega^{\pm}$ invariant mass distribution obtained by the DØ (CDF) collaboration, and taken from Ref. [41] ([39]), respectively. The control distribution of the $J/\psi\Xi^{\pm}$ invariant mass obtained by the CDF collaboration is also shown.

ing fractions are almost equal.[44, 45, 51] Since the soft photon from the decay $B^{*+} \to B^+\gamma$ is not reconstructed, these decays produce three visible peaks in the distribution of the mass difference $\Delta m = m(B^+\pi^-) - m(B^+)$, with the signal from the decays $B_1^0 \to B^{*+}\pi^-$ and $B_2^{*0} \to B^+\pi$ shifted from the nominal position by $\delta m = M(B^{*+}) - M(B^+) = 45.8$ MeV.

The DØ collaboration performed the analysis using 1.3 fb^{-1} of statistics.[52] The B^+ meson was selected in the decay mode $B^+ \to J/\psi K^+$ with $J/\psi \to \mu^+\mu^-$. The obtained distribution of the difference $m(B^+\pi^-) - m(B^+)$ is shown in the left plot in Fig. 8. The signal of the excited B mesons is clearly seen, although the separation of the three decay modes is quite difficult, and involves the theoretical assumption on the B_1 and B_2^* decay widths. The CDF collaboration used in their study[53] three decay modes of B^+, namely $B^+ \to J/\psi K^+$ with $J/\psi \to \mu^+\mu^-$, $B^+ \to \bar{D}^0\pi^+$, and $B^+ \to \bar{D}^0\pi^+\pi^-\pi^+$ with $\bar{D}^0 \to K^+\pi^-$. The distribution of the Q values defined as $Q = m(B^+\pi^-) - m(B^+) - m(\pi^-)$ is shown in the right plot in Fig. 8. The signal of the excited B mesons is also clearly seen and in a qualitative agreement with the result obtained by the DØ collaboration.

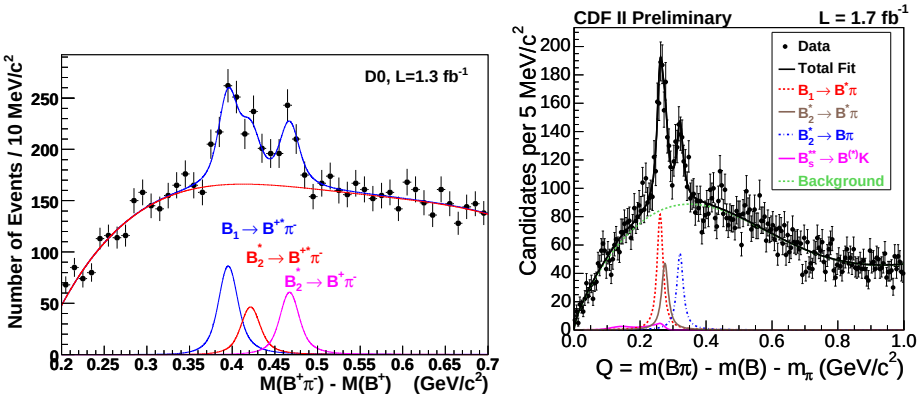

Figure 8: The left plot taken from Ref. [52] shows the invariant mass difference $m(B^+\pi^-) - m(B^+)$ for the exclusive B^+ decays obtained by DØ collaboration. The line shows the fit to the obtained distribution. The contribution of background and the three signal peaks are shown separately. The right plot taken from Ref. [53] shows the distribution of the mass difference $Q = m(B^+\pi^-) - m(B^+) - m(\pi^-)$ for exclusive B+ decays obtained by the CDF collaboration. Curves are shown separately for the background, the $B_s^{**} \to B^{(*)}K$ reflections, and the three decays of excited B mesons.

The DØ collaboration reports the following measured masses of B_1 and B_2^* mesons:

$$m(B_1) \quad = \quad 5720.6 \pm 2.4(\text{stat}) \pm 1.4(\text{syst}) \text{ MeV}, \tag{17}$$

$$m(B_2^*) \quad = \quad 5746.8 \pm 2.4(\text{stat}) \pm 1.7(\text{syst}) \text{ MeV}. \tag{18}$$

In addition, the following ratios were measured:

$$\frac{\text{Br}(B_1 \to B^* \pi)}{\text{Br}(B_1, B_2^* \to B^{(*)} \pi)} \quad = \quad 0.477 \pm 0.069(\text{stat}) \pm 0.062(\text{syst}); \tag{19}$$

$$\frac{\text{Br}(B_2^* \to B^* \pi)}{\text{Br}(B_2^* \to B^{(*)} \pi)} \quad = \quad 0.475 \pm 0.095(\text{stat}) \pm 0.069(\text{syst}); \tag{20}$$

$$\frac{\text{Br}(b \to (B_1, B_2^*) \to B^{(*)+} \pi^-)}{\text{Br}(b \to B^+)} \quad = \quad 0.139 \pm 0.019(\text{stat}) \pm 0.032(\text{syst}). \tag{21}$$

The CDF collaboration found the masses of B_1 and B_2^* mesons to be equal to

$$m(B_1) \quad = \quad 5725.3^{+1.6}_{-2.2}(\text{stat})^{+1.4}_{-1.5}(\text{syst}) \text{ MeV}, \tag{22}$$

$$m(B_2^*) \quad = \quad 5740.2^{+1.7}_{-1.8}(\text{stat})^{+0.9}_{-0.8}(\text{syst}) \text{ MeV}. \tag{23}$$

In addition, they measured the natural width of the B_2^* meson, which is found to be

$$\Gamma(B_2^{*0}) = 22.7^{+3.8}_{-3.2}(\text{stat})^{+3.2}_{-10.2}(\text{syst}) \text{ MeV}. \tag{24}$$

The masses measured by both experiments are in a reasonably good agreement between them and with the theoretical predictions.

3.8 Excited B_s mesons

The $(b\bar{s})$ system should reveal the same pattern of the excited mesons as the $(b\bar{d})$ system. The quark theory predicts the existence of two broad states B_{s0}^* and B_{s1}^*, and two narrow states B_{s1} and B_{s2}^*. The narrow states can be observed experimentally. The B_{s1} meson can only decay to $B_{s1} \to B^* K$, while B_{s2}^* meson can decay to both $B_{s2}^* \to B^* K$ and $B_{s2}^* \to BK$ final states. However, the decay $B_{s2}^* \to B^* K$ is strongly suppressed due to a small available phase space.

The CDF collaboration reconstructed the B^+ meson in the decays modes $B^+ \to J/\psi K^+$ with $J/\psi \to \mu^+\mu^-$, and $B^+ \to \bar{D}^0 \pi^+$ with $\bar{D}^0 \to K^+ \pi^-$. They analysed[54] the statistics collected with 1 fb^{-1} of $p\bar{p}$ collisions. The obtained distribution of the difference $m(B^+K^-) - m(B^+) - m(K-)$ is shown in the left plot in Fig. 9. The signal corresponding to the decays $B_{s1} \to B^{*+}K^-$ and $B_{s2}^* \to B^+K^-$ are clearly seen. The statistical significance of each of the signals exceeds five standard deviations. The result of the similar study[55] reported by the DØ collaboration is shown in the right plot in Fig. 9. They used the decay $B^+ \to J/\psi K^+$ with $J/\psi \to \mu^+\mu^-$ in their analysis. The DØ collaboration observes the signal of the $B_{s2}^* \to B^+K^-$ decay with the statistical significance exceeding 5 standard deviations, but they were not able to stated any conclusive statement on the $B_{s1} \to B^{*+}K^-$ decay due to the insufficient significance of the possible signal.

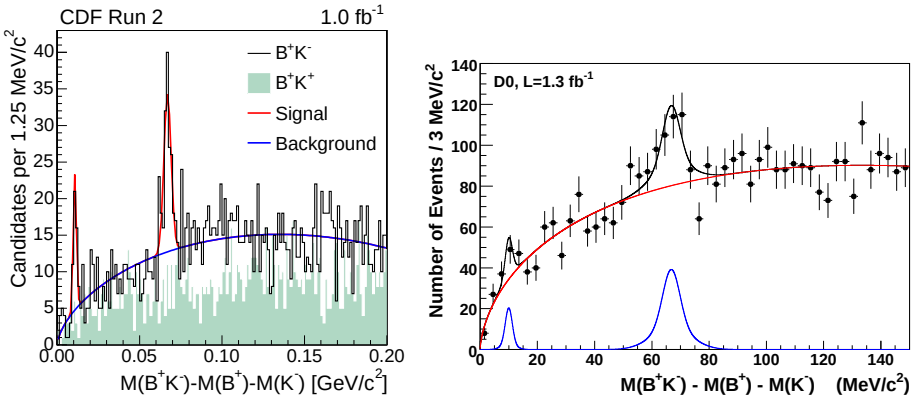

Figure 9: The left plot taken from Ref. [54] shows the distribution of $Q = m(B^+K^-) - m(B^+) - m(K-)$ obtained by the CDF collaboration for both B^+ channels combined. The dotted line shows the result of a fit with the sum of a background function and two Gaussians. The filled area shows the Q distribution for the wrong-sign combination B^+K+. The right plot taken from Ref. [55] shows the invariant mass difference $m(B^+K^-) - m(B^+) - m(K-)$ for exclusive B^+ decays obtained by the DØ collaboration. The line shows the fit with a two-peak hypothesis. Shown separately are contributions from signal and background.

The masses of B_{s1} and B^*_{s2} mesons measured by the CDF collaboration are found to be

$$m(B_{s1}) = 5829.4 \pm 0.2(\text{stat}) \pm 0.1(\text{syst}) \pm 0.6(\text{PDG}) \text{ MeV}, \quad (25)$$
$$m(B^*_{s2}) = 5839.6 \pm 0.4(\text{stat}) \pm 0.1(\text{syst}) \pm 0.5(\text{PDG}) \text{ MeV}. \quad (26)$$

The last uncertainty in these results is due to the uncertainty of different values taken from the Particle Data Group [56].

The mass of the B^*_{s2} meson obtained by the DØ collaboration is

$$m(B^*_{s2}) = 5839.6 \pm 1.1(\text{stat}) \pm 0.7(\text{syst}) \text{ MeV}. \quad (27)$$

In addition, the DØ collaboration measured the production rate of B^*_{s2} meson

$$\frac{\text{Br}(b \to B^*_{s2} \to B^+K^-)}{\text{Br}(b \to B^+)} = (1.15 \pm 0.23(\text{stat}) \pm 0.13(\text{syst}))\%. \quad (28)$$

The results of two collaborations agree very well between them.

3.9 Conclusions

Concluding this section, it can be stated that the experiments at the Tevatron obtained the impressive results on the spectroscopy of the B hadrons. Many objects were observed for the first time and their measured parameters provide an important input for improving and developing the theoretical models describing the bound states of quarks. Still, many B hadrons, like the baryons containing two or three b quarks, need to be discovered, and the experiments at the LHC collider have many possibilities to contribute in this exciting direction of B physics.

4 Lifetime of B hadrons

The lifetime is one of the most important properties of hadron. It is determined by the interplay of the strong interaction which bounds quarks together, and the weak interaction responsible for the transition of one quark type to another. Therefore measuring the lifetime provides an important information on the underlying theory of strong interactions (QCD) and helps to develop the numerical models used to predict the B-hadron lifetime.

A large mass of b quark significantly simplifies the computation of the B-hadron lifetime, since the QCD at the energy corresponding to $m(b) = 4.12 \pm 0.03$ GeV[14] becomes a perturbative theory, so that its predictions become precise and unambiguous with small theoretical uncertainties. According to this prediction, the lifetimes of stable B hadrons should exhibit the following striking hierarchy:

$$\tau(B^+) > \tau(B^0) \approx \tau(B^0_s) > \tau(\Lambda_b) \gg \tau(B_c) \quad (29)$$

The lifetime of all B hadrons, except the lifetime of B_c meson, should be the same within 10%, while the lifetime of the B_c meson should be considerably smaller. The experimental task is to verify this prediction. Until the start of the LHC experiments, essentially all what was known about the B-hadron lifetimes, except the lifetimes of B^+ and B^0 mesons, came from the Tevatron experiments. And even for B^+ and B^0 mesons, the CDF and DØ experiments provide an important contribution in the world average values, because the accuracy achieved by them is comparable to the results of the b-factory experiments.

The theoretical prediction is more precise for the ratio of lifetimes of two B hadrons. For example, the ratio of B_s^0 and B^0 lifetimes is predicted with the theoretical uncertainty of the order of 1%. Form the experimental point of view, the measurement of the ratio of lifetimes is also often more precise than the measurement of the individual lifetimes, because many systematic uncertainties cancel in the corresponding ratio. Therefore, the comparison of the theoretical and experimental results on the lifetime ratios is the most meaningful and educative, and in this section we will pay a special attention to the experimental results on the lifetime ratios.

4.1 B^+ and B^0 lifetimes

The CDF collaboration performed several measurements of the B^+ and B^0 lifetimes. The most precise result comes from the study of B hadron decays involving $J/\psi \to \mu^+\mu^-$ final state.[57] This final state can be selected using the di-muon trigger without applying the lifetime biasing cuts. Using the statistics corresponding to an integrated luminosity of 4.3 fb^{-1}, the CDF collaboration collected 43000 ± 230 decays $B^+ \to J/\psi K^+$, 16860 ± 140 decays $B^0 \to J/\psi K^{*0}$ and 12070 ± 120 decays $B^0 \to J/\psi K_s^0$. For each collected sample the lifetime of B^+ and B^0 mesons is obtained using an unbinned maximum likelihood fit. The corresponding likelihood function L is multivariate, and is based on the probability of observing a given candidate with reconstructed mass, decay time, decay time uncertainty, and mass uncertainty. The comparison of the decay time distribution and the projections of the likelihood function after the fit is shown in Fig. 10. It can be seen that the quality of the description of data is good.

Using the collected statistics, the CDF collaboration obtained the following results:

$$\tau(B^+) = 1.639 \pm 0.009(\text{stat}) \pm 0.009(\text{syst}) \text{ ps}, \quad (30)$$

$$\tau(B^0) = 1.507 \pm 0.010(\text{stat}) \pm 0.008(\text{syst}) \text{ ps}. \quad (31)$$

These results are consistent and have the similar precision as the corresponding measurement by Belle collaboration.[58] The ratio of lifetimes of B^+ and B^0 mesons provides an interesting possibility of comparison with the theoretical prediction, which is very precise due to the cancelation of many theoretical uncertainties. On the other hand, the systematic uncertainty of the experimental result is also reduced in the ratio of the lifetimes. The ratio of lifetimes

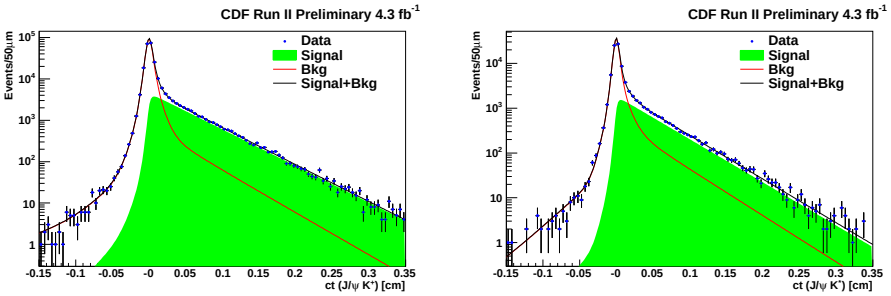

Figure 10: Decay time distributions for $B^+ \to J/\psi K^+$ (left plot) and $B^0 \to J/\psi K^{*0}$ (right plot) candidates taken from Ref. [57]. The decay time projection of the likelihood function is shown overlaid.

$\tau(B^+)/\tau(B^0)$ found by the CDF collaboration is

$$\tau(B^+)/\tau(B^0) = 1.088 \pm 0.009(\text{stat}) \pm 0.004(\text{syst}). \tag{32}$$

The theoretical prediction[59, 60, 61, 62, 63, 64, 65] of this ratio is in the range $1.04 - 1.08$, which is consistent with this experimental ratio.

The DØ collaboration performed an original direct measurement[66] of the ratio of the lifetimes of B^+ and B^0 mesons using the semileptonic decays $B^+ \to \mu^+\nu\bar{D}^0X$ and $B^0 \to \mu^+\nu D^{*-}$ with $D^{*-} \to \bar{D}^0\pi$ and $\bar{D}^0 \to K^+\pi^-$. Using just 440 pb^{-1} of $p\bar{p}$ collisions, the DØ collaboration collected more than 120000 events containing $\mu^+\bar{D}^0$ final state. Since the neutrino in the decays of B mesons is not reconstructed, the proper decay length can not be determined. Therefore, the DØ collaboration defined the visible proper decay length ($VPDL$) using the measured decay length in the laboratory frame and the total reconstructed momentum of the $\mu^+\bar{D}^0$ or μ^+D^{*-} system. They measured the ratio R of the number of μ^+D^{*-} and $\mu^+\bar{D}^0$ events as a function of the $VPDL$. If the lifetime of the B^+ and B^0 mesons is different, the ratio R should change with the change of the $VPDL$. Namely this variation is observed experimentally, as it can be seen in Fig. 11, and from the shape of this variation the ratio $\tau(B^+)/\tau(B^0)$ can be extracted. Since the final states $\mu^+\bar{D}^0$ or μ^+D^{*-} are very similar and can be selected using almost the same criteria, many experimental uncertainties cancel in this $\tau(B^+)/\tau(B^0)$ measurement. Using this method, the DØ collaboration obtained the value

$$\tau(B^+)/\tau(B^0) = 1.080 \pm 0.016(\text{stat}) \pm 0.014(\text{syst}). \tag{33}$$

This result agrees with the theoretical expectations and with the other measurements of this quantity.

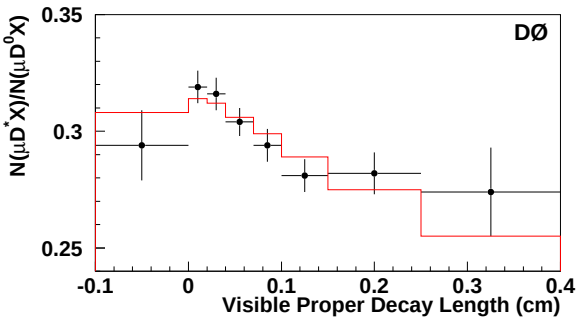

Figure 11: Points with the error bars show the ratio of the number of events in the $\mu^+ D^{*-}$ and $\mu^+ \bar{D}^0$ samples as a function of the visible proper decay length. The result of the fit of this distribution with $\tau(B^+)/\tau(B^0) = 0.080$ is shown as a histogram. The plot is taken from Ref. [66].

4.2 B_s^0 lifetime

B_s^0 meson system, like any other neutral meson, contains the short-lived and and long-lived states. They differ by mass and lifetime and are denoted as the light (B_L) and heavy (B_H) states, respectively, with the value of $\Delta\Gamma = \Gamma_L - \Gamma_H$ to be positive in the SM. Since the value of $\Delta\Gamma_s$ is relatively large, the measured lifetime of the B_s system depends on the B_s^0 decay mode in which it is measured. The distinctive cases are the flavor specific final state, the $B_s^0 \to J/\psi\phi$ decay, which is a mixture of CP-even and CP-odd final state, and CP-specific final state, like the $B_s^0 \to J/\psi f_0(980)$ decay. The Tevatron collaborations contributed in the measurement of the B_s^0 lifetime in all these final states, and the precision of their measurements was the world best until the start of the LHC experiments.

The flavour specific lifetime of the B_s^0 system is measured by the DØ collaboration[67] in the semileptonic decay $B_s^0 \to \mu^+ D_s^- X$. Using just 400 pb^{-1} of available statistics, they reconstructed about 5000 decays $B_s^0 \to \mu^+ D_s^- X$ and measured the B_s^0 lifetime to be

$$\tau(B_s^0 \to \mu^+ D_s^- X) = 1.398 \pm 0.044(\text{stat})^{+0.028}_{-0.025}(\text{syst}) \text{ ps}. \quad (34)$$

Figure 12 shows the distribution of the pseudo proper decay length, which is another name of VPDL introduced before, of the reconstructed $B_s^0 \to \mu^+ D_s^- X$ decays together with the result of the log likelihood fit superimposed. In general, there is an excellent description of the observed data with the χ^2 per degree of freedom (dof) $\chi^2/dof = 1.06$. This result has a potential of considerable improvement, since less than 5% of the final statistics is used in the analysis, but the DØ collaboration never updated it. Nevertheless, even with

such a small statistics this result remains one of the most precise flavour specific measurements of the B_s^0 lifetime.

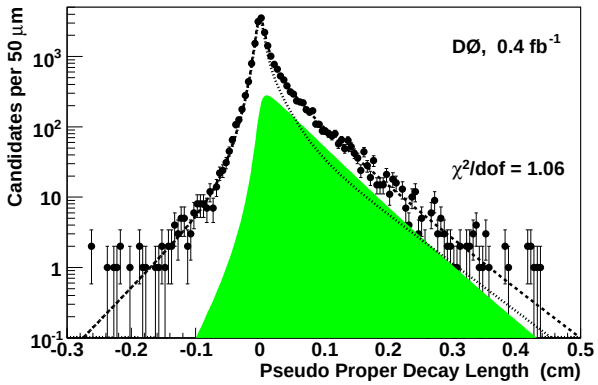

Figure 12: Pseudo-proper decay length distribution for $\mu^+ D_s^-$ candidates with the result of the fit superimposed as the dashed curve. The dotted curve represents the combinatorial background and the filled area represents the B_s^0 signal. The plot is taken from Ref. [67].

The CDF collaboration measured[68] the flavor-specific lifetime of B_s^0 meson using the decay $B_s^0 \to D_s^- \pi^+(X)$ with $D_s^- \to \phi\pi^-$ and X representing possible additional particles which are not reconstructed. The statistics used in this analysis corresponds to 1.3 fb^{-1} integrated luminosity of $p\bar{p}$ collisions. Fig. 13 shows the invariant mass dstribution of selected $D_s^- \pi^+$ candidates. The CDF collaboration includes in the measurement the exclusive decays of B_s^0, seen in Fig. 13 as the narrow peak, and partially reconstructed B_s^0 decays, seen as a bump on the left side from the peak. This addition allowed to more than double the number of B_s^0 decays used in the analysis, although adding some difficulties in treatment of the partially reconstructed B_s^0 decays. It can be seen from Fig. 13 that there is a very good understanding of the observed invariant mass distribution and all essential decay modes of B hadrons are included in the analysis.

Using the selected sample of B_s^0 decays, the CDF collaboration obtained the following flavour specific B_s^0 lifetime:

$$\tau(B_s^0 \to D_s^- \pi^+(X)) = 1.518 \pm 0.041(\text{stat}) \pm 0.027(\text{syst}) \text{ ps}. \qquad (35)$$

The B_s^0 lifetime in the decay mode $B_s^0 \to J/\psi\phi$ is obtained from the full angular analysis including the measurement of the lifetime difference $\Delta\Gamma_s$ and the possible CP-violating phase ϕ_s and is described in Section 7 of this review.

The CDF collaboration also performed the measurement[69] of the B_s^0 lifetime in the pure CP-odd final state $B_s^0 \to J/\psi f_0(980)$. Neglecting the CP

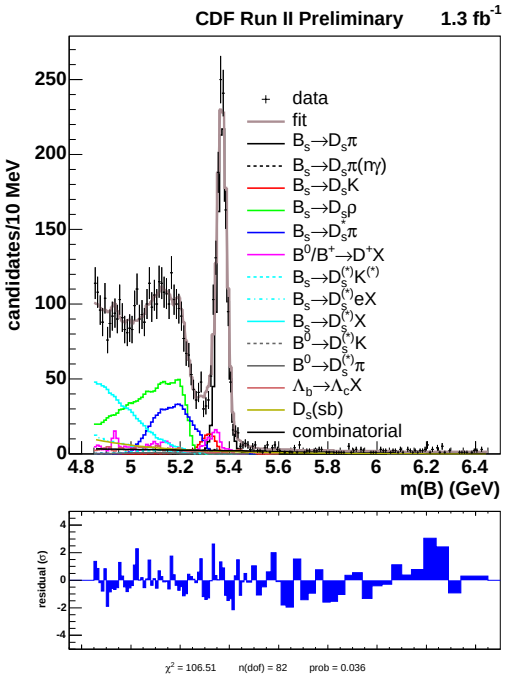

Figure 13: Invariant mass distribution for candidates reconstructed as $B_s^0 \to D_s^- \pi^+$ with fit projection overlaid. The plot is taken from Ref. [68].

violation, which is predicted to be very small in the SM, the B_s^0 lifetime in this mode should correspond to the lifetime of the B_s^H state. The CDF collaboration reconstructed 502 ± 37 such decays and used this statistics to measure the B_s^0 lifetime:

$$\tau(B_s^0 \to J/\psi f_0(980)) = 1.70^{+0.12}_{-0.11}(\text{stat}) \pm 0.03(\text{syst}) \text{ ps}. \quad (36)$$

At the time of the publication, it was the first measurement of the B_s^0 lifetime in a decay to CP eigenstate.

4.3 B_c^- lifetime

The lifetime of B_c^- meson should be much less than the lifetime of all other B mesons because both b and $\bar{c}$ quarks in B_c^- meson decay weakly and, in addition, these spectator quarks can annihilate. Within different theoretical approaches, the B_c^- lifetime is predicted to be[70, 71, 72, 73] in the range $0.36 - 0.53$ ps. Currently, all what we know about the B_c^- lifetime comes from the Tevatron experiments.

The CDF collaboration measured[74] the B_c^- lifetime using its semileptonic decay $B_c^- \to J/\psi l^- \bar{\nu}$, where l^- can be either an electron or a muon and $J/\psi \to \mu^+\mu^-$. They obtained

$$\tau(B_c^-) = 0.475^{+0.053}_{-0.049}(\text{stat}) \pm 0.018(\text{syst}) \text{ ps}. \quad (37)$$

In addition, the CDF collaboration measured[75] the B_c^- lifetime in the exclusive decay mode $B_c^- \to J/\psi\pi^-$ with $J/\psi \to \mu^+\mu^-$. They reconstructed 272 exclusive B_c^- decays using the integrated luminosity 6.7 fb^{-1}. Figure 14 shows the proper decay length distribution of selected $B_c^- \to J/\psi\pi^-$ candidates with the result of the fit superimposed. Using this sample of events, the CDF collaboration measured

$$\tau(B_c^-) = 0.452 \pm 0.048(\text{stat}) \pm 0.027(\text{syst}) \text{ ps}. \quad (38)$$

The DØ collaboration measured[76] the B_c^- lifetime using the semileptonic decay $B_c^- \to J/\psi\mu^-\bar{\nu}$ with $J/\psi \to \mu^+\mu^-$. They used the statistics corresponding to the integrated luminosity 1.3 fb^{-1} and reconstructed 881 ± 80 B_c^- candidates. The $VPDL$ distribution of selected candidates is shown in Fig. 15. The resulting B_c^- lifetime is found to be

$$\tau(B_c^-) = 0.448^{+0.038}_{-0.036}(\text{stat}) \pm 0.032(\text{syst}) \text{ ps}. \quad (39)$$

All results on B_c^- lifetime obtained by both collaboration are consistent with each other and with the theoretical predictions[70, 71, 73].

4.4 Lifetime of B baryons

Study of the B-baryon lifetime provides a valuable information for development of the numerical theoretical models describing the quark systems. The lifetime

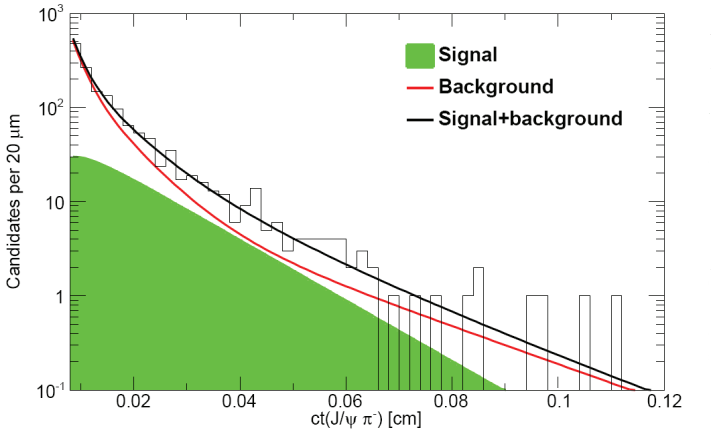

Figure 14: Decay-length distribution of $J/\psi\pi^-$ candidates taken from Ref. [75]. The fit projection, along individual contributions from signal and background, is overlaid.

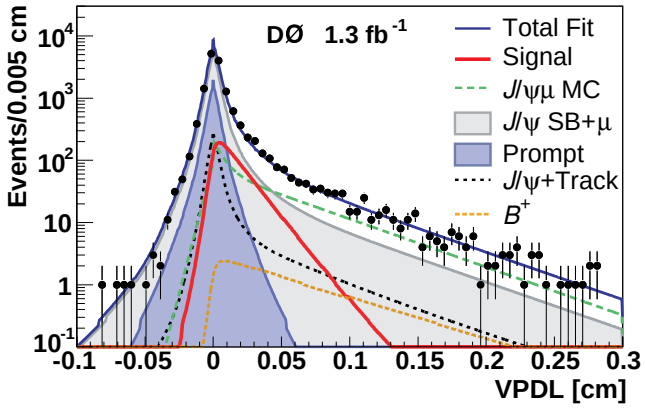

Figure 15: $VPDL$ distribution of the $J/\psi\mu$ sample with the projected components of the fit overlaid. The plot is taken from Ref. [76].

of Λ_b^0 baryon, containing (bud) quarks is predicted[64, 77] to be less than the lifetime of B^0 meson with $\tau(\Lambda_b^0)/\tau(B^0) = 0.92 \pm 0.03$. The early measurements[14] of Λ_b^0 lifetime from LEP were much less than the theoretical predictions, which explained an increased interest to the Λ_b^0 lifetime.

The DØ collaboration measured the Λ_b^0 lifetime both in the semileptonic and hadronic decay modes. For the first measurement[78] the semileptonic decay $\Lambda_b^0 \to \mu^- \bar{\nu} \Lambda_c^+$ is used with $\Lambda_c^+ \to K_S^0 p$. In total 4437 ± 329 such decays are reconstructed using the statistics corresponding to the integrated luminosity 1.3 fb^{-1}. The left plot in Fig. 16 shows the observed $VPDL$ distribution (denoted in Ref. [78] as λ^M) together with the result of the fit. The Λ_b^0 lifetime is found to be

$$\tau(\Lambda_b^0) = 1.290^{+0.119}_{-0.110}(\text{stat})^{+0.087}_{-0.091}(\text{syst}) \text{ ps}. \quad (40)$$

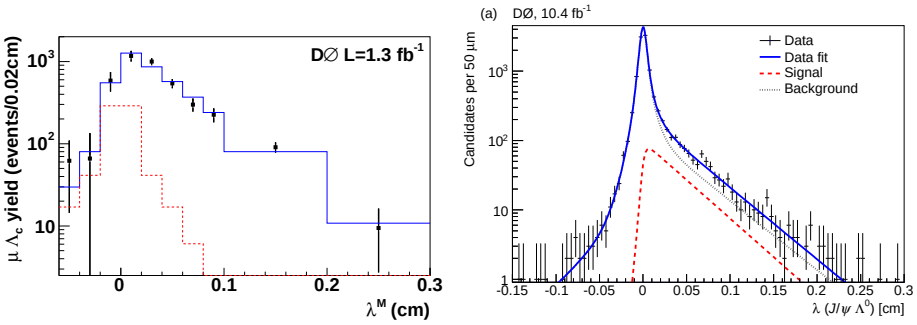

Figure 16: Left plot taken from Ref. [78]: Measured $\mu\Lambda_c$ yields in the $VPDL$ bins denoted as λ^M (points) and the result of the lifetime fit (solid histogram). The dashed histogram shows the contribution of peaking background. Right plot taken from Ref. [79]: Proper decay length distributions for $\Lambda_b^0 \to J/\psi\Lambda$ candidates, with fit results superimposed.

In the second measurement[79] of the Λ_b^0 lifetime by the DØ collaboration, the decay $\Lambda_b^0 \to J/\psi\Lambda$ with $J/\psi \to \mu^+\mu^-$ and $\Lambda \to K^- p$ was used. In total 755 ± 49 such decays were reconstructed using the full collected statistics corresponding to the integrated luminosity 10.4 fb^{-1}. The proper decay length distribution of selected candidates is shown in Fig. 16 (right plot). From this statistics the measured Λ_b^0 lifetime is found to be

$$\tau(\Lambda_b^0) = 1.303 \pm 0.075(\text{stat}) \pm 0.035(\text{syst}) \text{ ps}. \quad (41)$$

The most precise measurements of the Λ_b^0 lifetime by CDF collaboration were performed in hadronic decay modes. The analysis in Ref. [80] exploits the decay $\Lambda_b^0 \to \Lambda_c^+\pi^-$ with $\Lambda_c^+ \to pK^+\pi^-$. Like in all other measurements with hadronic decays of B hadrons, the special trigger on the displaced vertex

developed by the CDF collaboration is used. Since such a trigger biases the lifetime distribution, a special attention in this analysis was given to a correct reconstruction of the selection efficiency of Λ_b^0 candidates. It is obtained from the simulation of the trigger and detector, and is validated using $J/\psi \to \mu^+\mu^-$ decays.

In total 2905 ± 58 decays $\Lambda_b^0 \to \Lambda_c^+\pi^-$ were reconstructed using the full collected statistics corresponding to the integrated luminosity 1.1 fb^{-1}. The reconstructed proper decay length of Λ_b^0 candidates together with the result of the fit is shown in Fig. 17 (left plot). It can be seen that a very good description of the reconstructed data, including a complicated trigger efficiency is achieved. The measured Λ_b^0 lifetime is

$$\tau(\Lambda_b^0) = 1.401 \pm 0.046(\text{stat}) \pm 0.035(\text{syst}) \text{ ps}. \tag{42}$$

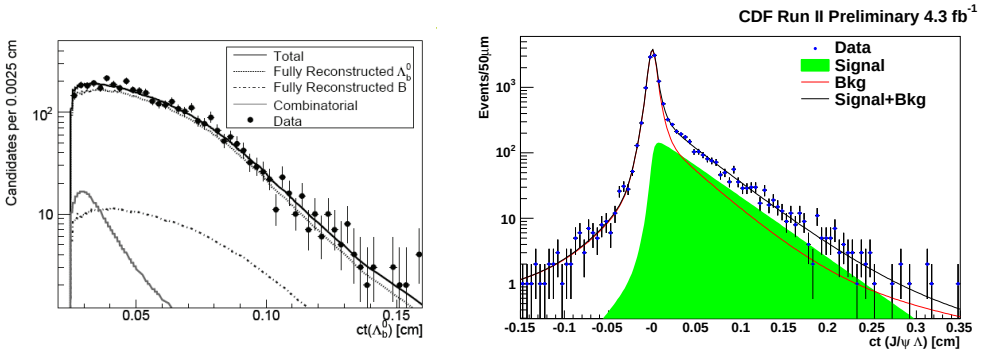

Figure 17: Left plot taken from Ref. [80]: The distribution of the proper decay length ($c\tau$) of $\Lambda_b^0 \to \Lambda_c^+\pi^-$ candidates (points) with the fit projection overlaid (solid black line). Right plot taken from Ref. [57]: The proper decay length ($c\tau$) distribution for $\Lambda_b^0 \to J/\psi\Lambda$ candidates.

Another measurement[57] of Λ_b^0 lifetime by the CDF collaboration is done in the decay mode $\Lambda_b^0 \to J/\psi\Lambda$ with $J/\psi \to \mu^+\mu^-$ and $\Lambda \to K^+\pi^-$. This analysis uses the statistics corresponding to the integrated luminosity of 4.3 fb^{-1}. The analysis technique in this decay mode is straightforward and similar to the corresponding measurement[79] by the DØ collaboration. In total 1710 ± 50 Λ_b^0 decays were reconstructed. The proper decay length distribution is shown in Fig. 17 (right plot). The measured Λ_b^0 lifetime is found to be

$$\tau(\Lambda_b^0) = 1.537 \pm 0.045(\text{stat}) \pm 0.014(\text{syst}) \text{ ps}. \tag{43}$$

The obtained Λ_b^0 lifetime is 3.4 standard deviation larger than the world average computed excluding this result. Therefore, additional measurements of the Λ_b^0 lifetime are required to resolve this ambiguity.

In addition to Λ_b^0 lifetime, the CDF collaboration also measured[39] the lifetime of Ξ_b^- and Ω_b^- baryons. The obtained values are

$$\tau(\Xi_b^-) = 1.56^{+0.27}_{-0.25}(\text{stat}) \pm 0.02(\text{syst}) \text{ ps.} \quad (44)$$

$$\tau(\Omega_b^-) = 1.13^{+0.53}_{-0.40}(\text{stat}) \pm 0.02(\text{syst}) \text{ ps.} \quad (45)$$

The precision of these measurements is not sufficient to make any conclusion on a possible variation of the lifetime of different B baryons, so that more precise measurements at LHC are required to clarify the lifetime pattern in B baryons.

4.5 Comparison with theoretical predictions and conclusions

The results on the lifetime of different B hadrons obtained at the Tevatron provide a very interesting possibility to verify the theoretical predictions. The most accurate values predicted by the theoretical models are given for the ratios of B-hadron lifetimes relative to the B^0 lifetime, and namely the comparison of these ratios is shown in Table 2. The world average experimental results and the theoretical predictions given in this Table are taken from Ref. [81].

Table 2: Measured ratios of B-hadron lifetimes relative to the B^0 lifetime and ranges predicted by theory.

Lifetime ratio	Measured value	Predicted range
$\tau(B^+)/\tau(B^0)$	1.079 ± 0.007	$1.04 - 1.08$
$\tau(B_s^0)/\tau(B^0)$	0.993 ± 0.009	$0.99 - 1.01$
$\tau(\Lambda_b^0)/\tau(B^0)$	0.930 ± 0.020	$0.86 - 0.95$
$\tau(B_c^+)/\tau(B^0)$	0.302 ± 0.020	$0.24 - 0.35$

There is a striking agreement between the experiment and the theory for all types of B hadrons. The experiments confirm the expected pattern of B-hadron lifetimes given in Eq. (29). It can also be noticed that the experimental precision is currently better for all B hadrons, which opens an excellent opportunity of improving the theoretical computations. Many Tevatron results were obtained with a small part of the available statistics, so that the precision of many Tevatron measurements could be significantly improved. However, the lack of manpower will probably prevent to achieve this improvement. Nevertheless, it is important to stress that the contribution of the Tevatron results, even without adding more statistics, is dominant or essential for the precision of all measured B-hadron lifetimes. Thus, the lifetimes of B hadrons is a very important achievement and a long-lasting legacy of the CDF and DØ experiments.

5 $B_s^0 - \bar{B}_s^0$ mixing

All neutral ground state mesons (K^0, D^0, B^0, B_s^0) can change their flavor from particle to antiparticle during the lifetime. This phenomenon is called an oscillation. The B^0 oscillations was well established before the experiments at the Tevatron[81], with a precisely measured oscillation frequency Δm_d. In the SM, the parameter Δm_q of B_q^0 meson, where where $q = d, s$, is proportional to the combination $|V_{tb}^* V_{tq}|^2$ of Cabibbo-Kobayashi-Maskawa (CKM) matrix elements[14]. Since the matrix element V_{ts} is larger than V_{td}, the frequency Δm_s is higher, which makes it very difficult to detect. As a result, the B_s^0 oscillation have not been observed by any previous experiment. However, Δm_s is a crucial parameter for establishing the unitarity relation of the CKM matrix. Its measurement yields the ratio $|V_{ts}/V_{td}|$, which has a smaller uncertainty than $|V_{td}|$ alone due to the cancellation of certain theory uncertainties and provides a stringent constraint on the unitarity triangle and the source of CP violation in the SM[14, 82, 83, 84].

The measurement of the oscillation frequency is very complicated, since it requires the identification of both initial and final state of the B_s^0 meson and the detection of the time evolution of oscillated events. The DØ collaboration used for this purpose[85] the semileptonic $B_s^0 \to \mu + D_s^- X$ decays with $D_s^- \to \phi\pi^-$. The analysed statistics corresponds to the integrated luminosity of 1 fb^{-1}. They collected 26700 ± 556 candidates.

The final flavor of B_s meson in this decay mode is determined by the charge of the muon. The initial flavor tagging is more involved. Its quality is described by the tagging power P, which is defined as $P = \varepsilon(2f_R - 1)^2$, where ε is the efficiency to select the tagged events and f_R is the fraction of events with correct identification of the initial flavor relative to the total number of tagged events. The tagging power P multiplied by the total number of selected events corresponds to the effective statistics used in the measurement of oscillation frequency.

The DØ collaboration developed a sophisticated initial flavor tagging technique[86]. It is based on the measurement of the flavor of the complementary B hadron in the pair production $B_s^0 \bar{B}$ or $\bar{B}_s^0 b$. Its flavour is correlated with the initial flavour of B_s^0 meson. This technique is called the opposite-side flavor tagging. The DØ collaboration achieved the tagging power

$$P = (2.48 \pm 0.21(\text{stat})^{+0.08}_{-0.06}(\text{syst})) \times 10^{-2}. \tag{46}$$

The flavor-tagged events were used in an unbinned fitting procedure. The likelihood, $\mathcal{L}$, for an event to arise from a specific source of the signal or background was determined event-by-event. This likelihood depends on the measured decay length, its uncertainty , the invariant mass of the candidate $m(K^+K^-\pi^-)$, the predicted value of f_R, and the purity of the signal selection. The resulting amplitude of B_s^0 oscillation as a function of Δm_s is shown in Fig. 18. The amplitude $A = 1$ corresponds to the B_s^0 oscillation, and the amplitude $A = 0$ corresponds to the absence of oscillation. Using the selected statistics and

the initial flavor tagging, the DØ collaboration determined the 90% confidence level interval of the B_s^0 oscillation frequency

$$17 < \Delta m_s < 21 \text{ ps}^{-1} \text{ (90\% C.L.)}. \tag{47}$$

At the time of publication it was the first double-sided bound on this quantity.

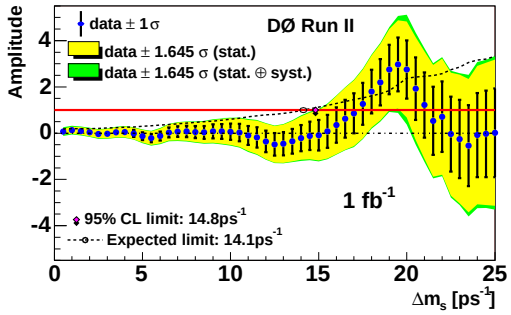

Figure 18: B_s^0 oscillation amplitude as a function of oscillation frequency, Δm_s, taken from Ref. [85]. The solid line shows the $A = 1$ axis for reference. The dashed line shows the expected limit including both statistical and systematic uncertainties.

The CDF collaboration searched for the B_s^0 oscillation in both semileptonic and hadronic final state.[87] They used the statistics corresponding to 1 fb^{-1} of $p\bar{p}$ collisions. The hadronic decays include $B_s^0 \to D_s^- \pi^+$ and $B_s^0 \to D_s^- \pi^+ \pi^- \pi^+$. The semileptonic decay mode used in the analysis is $B_s^0 \to l^+ D_s^- X$ ($l = \mu, e$). The D_s^- meson decays to three different final states $D_s^- \to \phi\pi^-$, $D_s^- \to K^{*0} K^-$, and $D_s^- \to \pi^+\pi^-\pi^-$ was used. In addition, the partially reconstructed hadronic decays with one or two photons missing were included in the analysis. These decays are $B_s^0 \to D_s^{*-}\pi$, $D_s^{*-} \to D_s^-\pi$ and $B_s^0 \to D_s^- \rho^+$, $\rho^+ \to \pi^+\pi^0$ with $D_s^- \to \phi\pi^-$. Their addition significantly increases the statistics, which is essential for this analysis. In total, 5600 fully reconstructed hadronic B_s^0 decays, 3100 partially reconstructed hadronic B_s^0 decays and 61500 partially reconstructed semileptonic B_s^0 decays were selected. Figure 19 shows the invariant mass distribution of $B_s^0 \to \mu^+ D_s^- X$ (left plot) and $B_s^0 \to D_s^- \pi^+$ (right plot) candidates. This plots show the contribution of different channels in the selected event samples. They also demonstrate an excellent understanding of the sample composition achieved in this analysis.

The fully and partially reconstructed hadronic decays give an important advantage to the CDF analysis. The precision of the proper decay time reconstruction is much better for these decays than for the semileptonic decays. The comparison of this precision for different decay types is shown in Fig. 20 taken

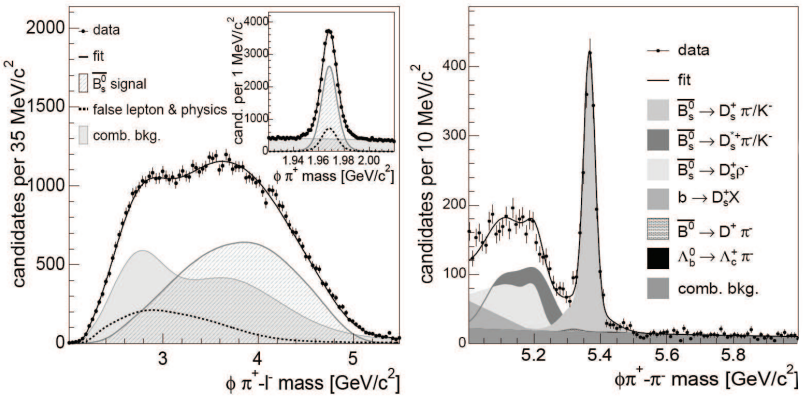

Figure 19: (Left panel) The invariant mass distributions for the $D_s^+ \to \phi\pi^+$ candidates [inset] and the $l^- D_s^+(\phi\pi^+)$ pairs. The contribution labelled "false lepton & physics" refers to backgrounds from hadrons mimicking the lepton signature combined with real D_s mesons and physics backgrounds such as $B^0 \to D_s^+ D^-$, $D_s^+ \to \phi\pi^+$, $D^- \to l^- X$. (Right panel) The invariant mass distribution for $\bar{B}_s^0 \to D_s^+(\phi\pi^+)\pi^-$ decays including the contributions from $\bar{B}_s^0 \to D_s^{*+}\pi^-$ and $\bar{B}_s^0 \to D_s^+\rho^-$. In this panel, signal contributions are drawn added on top of the combinatorial background. The plots are taken from Ref. [87].

from Ref. [87]. This precision is essential for the measurement of the B_s^0 oscillation. The B_s^0 meson changes flavor with high frequency, and namely this change needs to be detected. The value of $\Delta m_s = 17.5$ ps^{-1} corresponds to the period of oscillation in the proper decay time $\tau = 2\pi/\Delta m_s \simeq 360$ fs. The precision on this quantity should be at least 4 times better to measure the oscillation reliably. That is why the trigger on displaced tracks, allowing selection of the hadronic B_s^0 decays, played a crucial role in the successful detection of the B_s^0 oscillation by the CDF collaboration.

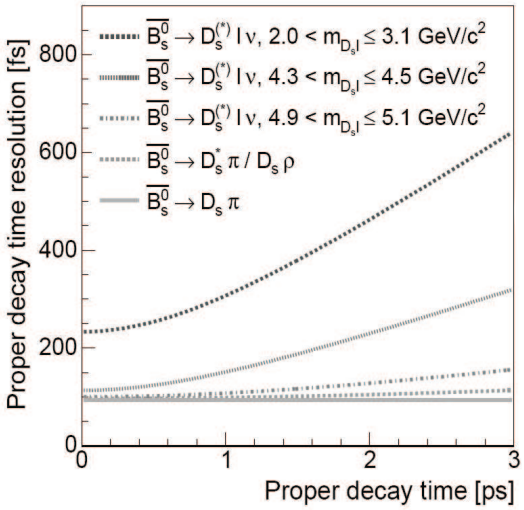

Figure 20: The average proper decay time resolution for B_s^0 decays as a function of proper decay time from Ref. [87].

Another important feature of this analysis is the application of both opposite-side and same-side flavor tagging. The B_s^0 meson is often accompanied by the charged kaon, produced during hadronisation of the initial b quark. Its charge corresponds to the initial flavor of the B_s^0 meson. Thus, by selecting this additional kaon and measuring its charge it is possible to determine the initial B_s^0 flavor. This technique is called the same-side flavor tagging. To implement it, the kaon needs to be identified among all other charged tracks. In the CDF analysis, the measurement of energy loss in the tracking detector and time-of-ight information are used to identify the kaons. The tagging power $P = 3.7\%(4.8\%)$ is achieved for the same-side tagging in hadronic (semi-leptonic) decay sample. The fractional uncertainty on P is approximately 25%. The opposite-side tagging power in the CDF measurement is $P = 1.8 \pm 0.1\%$.

The CDF collaboration uses an unbinned maximum likelihood fit to search

for Bs oscillations. The likelihood combines mass, decay time, decay-time resolution, and flavor tagging information for each candidate, and includes terms for signal and each type of background. The resulting amplitude of B_s^0 oscillation as a function of Δm_s is shown in Fig. 21. It can be seen that the amplitude increases to $\mathcal{A} = 1.20 \pm 0.20$ in the region around $\Delta m_s = 17.75$ ps^{-1}. For all other values of Δm_s it is consistent with zero. Using the available statistics and the developed analysis the CDF collaboration was able to report the discovery of the B_s^0 oscillation. The measured oscillation frequency was found to be

$$\Delta m_s = 17.77 \pm 0.10(\text{stat}) \pm 0.07(\text{syst}) \ (ps)^{-1}. \tag{48}$$

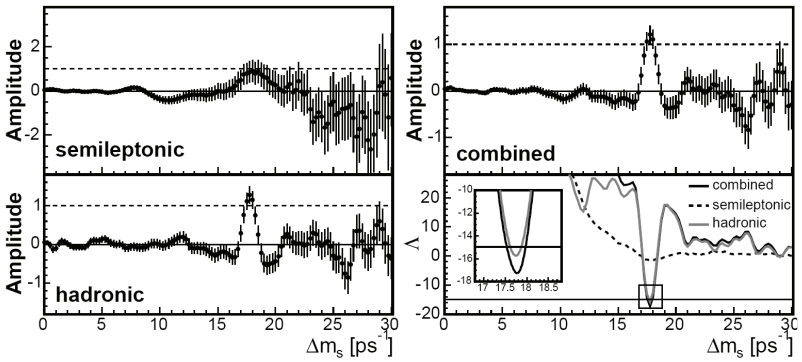

Figure 21: The measured amplitude values and uncertainties versus the $B_s^0 - \bar{B}_s^0$ oscillation frequency Δm_s taken from Ref. [87]. (Upper Left) Semileptonic decays only. (Lower Left) Hadronic decays only. (Upper Right) All decay modes combined. (Lower Right) The logarithm of the ratio of likelihoods for amplitude equal to one and amplitude equal to zero, $\Lambda = \log[\mathcal{L}^{A=0}/\mathcal{L}^{A=1}(\Delta m_s)]$, versus the oscillation frequency. The horizontal line indicates the value $\Lambda = 15$ that corresponds to a probability of 5.710^7 (5σ) in the case of randomly tagged data.

Figure 22 taken from Ref. [14] shows the impact of the Δm_s measurement on the unitarity test of the CKM matrix. It can be seen that this result provides one of the most strong constraints and is essential for verifying the unitarity of the CKM matrix. Thus, the measurement of the oscillation frequency at the Tevatron is one of the most important achievement of its B physics program.

6 Decays of B hadrons

The decays of B hadrons are very numerous and offer rich possibilities of various studies. It is impossible to cover all results in one review due to the size

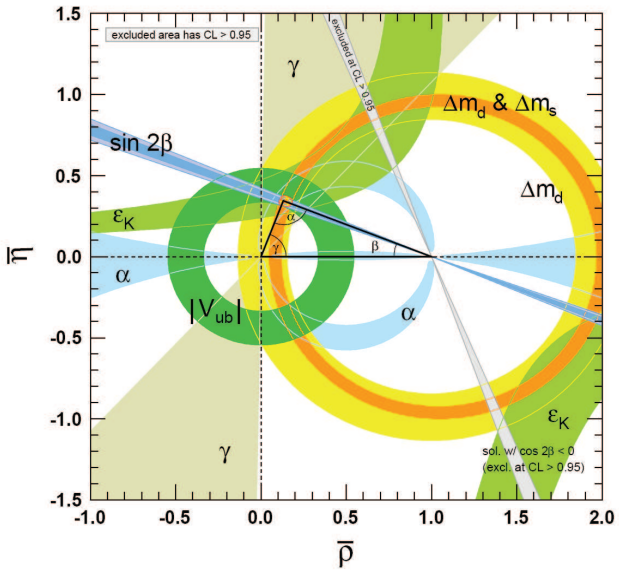

Figure 22: Constraints on the parameters of CKM matrix taken from Ref. [14]. The shaded areas have 95% confidence level.

limitations. We concentrate here on the most interesting results obtained at the Tevatron.

Probably the most important measurement in this research area is the search for the rare decays $B^0 \to \mu^+\mu^-$ and $B_s^0 \to \mu^+\mu^-$. These flavor-changing neutral current (FCNC) decays are forbidden in the SM at the tree level. Therefore, the SM predicts a very low value for the branching fractions of both $B^0 \to \mu^+\mu^-$ and $B_s^0 \to \mu^+\mu^-$ decays. The most recent SM prediction for these fractions is [88, 89, 90]

$$\begin{aligned} \mathrm{Br}(B_s^0 \to \mu^+\mu^-) &= (3.23 \pm 0.27) \times 10^{-9}, \\ \mathrm{Br}(B^0 \to \mu^+\mu^-) &= (1.07 \pm 0.10) \times 10^{-10}. \end{aligned} \tag{49}$$

The contribution of new physics beyond the SM can significantly modify these values.[91, 92, 93, 94] Thus, these rare decays can provide important constraints on various new physics models.

The DØ collaboration searched for these decays using 6.1 fb^{-1} of available statistics.[95] A multivariate neural network analysis was used to separate the possible signal from the background. Using this statistics, the following 95% confidence level upper limit on the branching fraction $B_s^0 \to \mu^+\mu^-$ was obtained:

$$\mathrm{Br}(B_s^0 \to \mu^+\mu^-) < 5.1 \times 10^{-9} \text{ at } 95\% \text{ C.L.} \tag{50}$$

The insufficient resolution of DØ tracking system did not allow to separate the possible contribution of $B^0 \to \mu^+\mu^-$ decay. Therefore, the above result was obtained assuming the SM value of $B^0 \to \mu^+\mu^-$ branching fraction.

The CDF collaboration presented in summer 2011 the analysis [96] with 7 fb^{-1} featuring an accumulation of signal-like events in the B_s^0 mass region with $\sim 2.5\sigma$ deviation from the background-only hypothesis. The latest CDF analysis,[97] which was still unpublished at the time of preparing this review, includes the full Run2 statistics corresponding to 9.6 fb^{-1}. Given the increased interest to the previous result, the analysis of the remaining statistics is kept the same. The separation between the signal and background in this analysis is achieved using the neural network. Figure 23 shows the observed and expected number of events in the $B_s^0 \to \mu^+\mu^-$ search for the different values of the neural network output variable ν_N. There is an excess of the signal-like events for $\nu_N > 0.97$, while the agreement between the observed and expected number of events is very good for the background-dominated region $\nu_N < 0.97$. The p-value of the SM signal plus background hypothesis for $\nu_n > 0.97$ is 7%. The excess of events in the $0.97 < \nu_N < 0.987$ bin is not increased with the addition of the new statistics and is consistent with the statistical fluctuation. The p-value of the SM signal plus background hypothesis for two largest ν_N bins is 22.4%, while the p-value of background only hypothesis is 2.1%. Thus, while still not conclusive, the experiment becomes sensitive to the SM contribution of $B_s^0 \to \mu^+\mu^-$ decay and shows a good agreement with the SM expectation.

The results obtained by the CDF collaboration with 9.6 fb^{-1} are:

$$\begin{aligned} \mathrm{Br}(B_s^0 \to \mu^+\mu^-) &= (1.3^{+0.9}_{-0.7}) \times 10^{-8}, \\ \mathrm{Br}(B^0 \to \mu^+\mu^-) &< 4.6 \times 10^{-9}\ (3.8 \times 10^{-9}) \text{ at } 95\%\ (90\%) \text{ C.L.} \end{aligned} \tag{51}$$

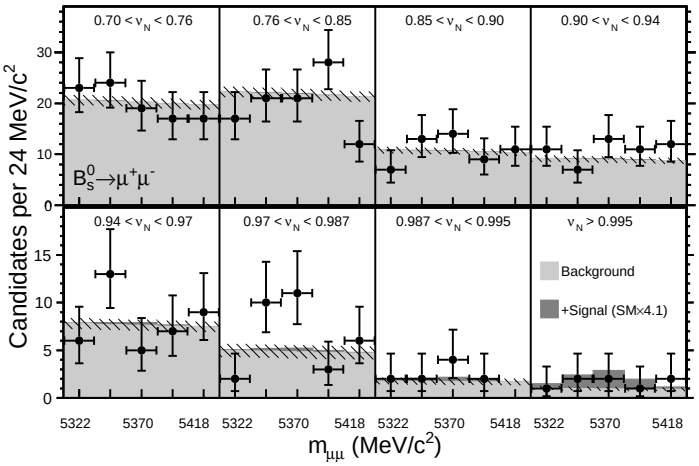

Figure 23: For the B_s mass region, the observed number of events (points) is compared to the total expected background (light grey) and its uncertainty (hatched) for different values of ν_N, taken from Ref. [97]. The hashed area represents the systematic uncertainty on the mean expected background while the error bars on the points represent the associated poisson uncertainty. Also shown is the expected contribution from $B_s^0 \to \mu^+\mu^-$ events (dark gray) using a branching fraction that corresponds to the central value from the fit to the data, which is 4.1 times the expected SM value.

The CDF collaboration also reports the first double sided limit on $\mathrm{Br}(B_s^0 \to \mu^+\mu^-)$:

$$\begin{aligned} 0.8 \times 10^{-9} < \quad & Br(B_s^0 \to \mu^+\mu^-) \quad < 3.4 \times 10^{-8} \text{ at } 95\% \text{ C.L.}, \\ 2.2 \times 10^{-9} < \quad & Br(B_s^0 \to \mu^+\mu^-) \quad < 3.0 \times 10^{-8} \text{ at } 90\% \text{ C.L.} \end{aligned} \tag{52}$$

The search of these rare decays continued at LHC and the LHCb collaboration reported recently the evidence of the $B_s^0 \to \mu^+\mu^-$ decay with the branching fraction consistent with the SM expectation:[98]

$$Br(B_s^0 \to \mu^+\mu^-) = (3.2^{+1.5}_{-1.2}) \times 10^{-9}. \tag{53}$$

The results of DØ and CDF are consistent with the value obtained by the LHCb collaboration. All these results are consistent with the SM prediction, providing a strong constraint on the contribution of the new physics processes.

The CDF collaboration performed an extensive study of the decays mediated by the FCNC transition $b \to s\mu^+\mu^-$ with different initial and final hadrons. The analysis is based on the statistics corresponding to 9.6 fb^{-1} of $p\bar{p}$ collisions. This result[99] was still unpublished at the time of preparing this report. In each case the branching fraction of the decay $H_b \to h\mu^+\mu^-$ is normalised to the well identified decay $H_b \to J/\psi h$ with $J/\psi \to \mu^+\mu^-$. Such a normalisation significantly reduces the systematic uncertainty of the measurements. The following results in different decay modes are obtained:

$$\mathrm{Br}(B^+ \to K^+\mu^+\mu^-) = [0.45 \pm 0.03(\mathrm{stat}) \pm 0.02(\mathrm{syst})] \times 10^{-6}, \tag{54}$$

$$\mathrm{Br}(B^+ \to K^{*+}\mu^+\mu^-) = [0.89 \pm 0.25(\mathrm{stat}) \pm 0.09(\mathrm{syst})] \times 10^{-6}, \tag{55}$$

$$\mathrm{Br}(B^0 \to K^0\mu^+\mu^-) = [0.33 \pm 0.08(\mathrm{stat}) \pm 0.03(\mathrm{syst})] \times 10^{-6}, \tag{56}$$

$$\mathrm{Br}(B^0 \to K^{*0}\mu^+\mu^-) = [1.14 \pm 0.09(\mathrm{stat}) \pm 0.06(\mathrm{syst})] \times 10^{-6}, \tag{57}$$

$$\mathrm{Br}(B_s^0 \to \phi\mu^+\mu^-) = [1.17 \pm 0.18(\mathrm{stat}) \pm 0.37(\mathrm{syst})] \times 10^{-6}, \tag{58}$$

$$\mathrm{Br}(\Lambda_b \to \Lambda\mu^+\mu^-) = [1.95 \pm 0.34(\mathrm{stat}) \pm 0.61(\mathrm{syst})] \times 10^{-6}. \tag{59}$$

Another interesting study performed at the Tevatron is the measurement of the branching fraction of the decay $B_s \to D_s^{(*)+} D_s^{(*)-}$. This decay is not rare, but it is expected that the final state is mainly CP-even and may saturate the total decay width of B_s^0 meson under certain theoretical assumptions.[100]

The DØ collaboration made an inclusive measurement of this branching fraction using 1.3 fb^{-1} of available statistics.[101] The decay $B_s \to D_s^{(*)+} D_s^{(*)-}$ was selected using the inclusive muon trigger. One D_s meson was partially reconstructed in the $D_s \to \mu\nu\phi$ decay mode. Another D_s meson was selected in $D_s \to \phi\pi$ decay mode. No attempt was made to distinguish D_s and D_s^* states. The resulting branching fraction is

$$\mathrm{Br}(B_s \to D_s^{(*)+} D_s^{(*)-}) = 0.039^{+0.019}_{-0.017}(\mathrm{stat})^{+0.016}_{-0.015}(\mathrm{syst}). \tag{60}$$

The CDF collaboration performed an analysis using 6.8 fb^{-1} of statistics.[102] They exclusively reconstructed all decay modes using the hadronic decays $D_s \to$

$\phi\pi$ or $D_s \to K^*K$. The resulting invariant mass distribution is presented in Fig. 24. In total 750 signal events in these decay modes are reconstructed. Using this statistics, the following result is obtained

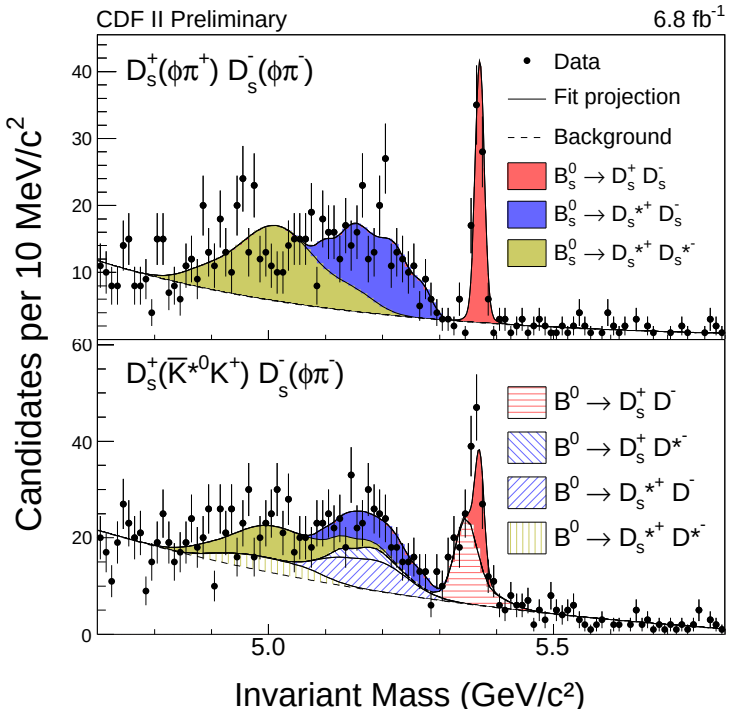

Figure 24: Invariant mass distribution of $B_s^0 \to D_s^+(\phi\pi^+)D_s^-(\phi\pi^-)$ and $B_s^0 \to D_s^+(K^{*0}K^+)D_s^-(\phi\pi^-)$. The plot is taken from Ref. [102].

$$Br(B_s^0 \to D_s^+ D_s^-) = (0.49 \pm 0.06(\text{stat}) \pm 0.05(\text{syst}) \pm 0.08(\text{norm}))\% \quad (61)$$
$$Br(B_s^0 \to D_s^{*\pm} D_s^{\mp}) = (1.13 \pm 0.12(\text{stat}) \pm 0.09(\text{syst}) \pm 0.19(\text{norm}))\% \quad (62)$$
$$Br(B_s^0 \to D_s^{*+} D_s^{*-}) = (1.75 \pm 0.19(\text{stat}) \pm 0.17(\text{syst}) \pm 0.29(\text{norm}))\% \quad (63)$$

The total branching fraction of these decay modes is found to be

$$Br(B_s^0 \to D_s^{(*)+} D_s^{(*)-}) = (3.38 \pm 0.25(\text{stat}) \pm 0.30(\text{syst}) \pm 0.56(\text{norm}))\%. \quad (64)$$

The results obtained by the CDF and DØ collaborations are consistent.

7 Study of CP asymmetry with B decays

An important part of B physics research at the Tevatron was devoted to the measurement of the CP asymmetry. Among other reasons, the interest to this

phenomenon is explained by the fact that the magnitude of the CP asymmetry included in the SM is not sufficient to describe the observed abundance of matter in our universe [103], which implies that some additional sources of CP asymmetry should exist. They could reveal themselves by deviating the observed CP asymmetry from the SM prediction. While the CP asymmetry in the decays of B^0 and B^+ mesons was extensively studied at B factories, the experiments at the Tevatron offer a possibility to study the CP violation in the decays of B_s^0 mesons. Until the start of the LHC era, it was the only place where such measurements were possible.

7.1 CP asymmetry in the decay $B_s^0 \to J/\psi\phi$

One of the most promising channels to search for the new sources of CP asymmetry is the decay $B_s^0 \to J/\psi\phi$. The CP asymmetry in this decay is described by the phase $\phi^{J/\psi\phi}$. Within the SM, this phase is related with the angle β_s of the (bs) unitarity triangle and is predicted to be very small [104]:

$$\phi_s^{J/\psi\phi}(SM) = -2\beta_s = -0.036 \pm 0.002. \tag{65}$$

This phase can be significantly modified by the new physics contribution and this deviation from the SM can be detected experimentally.

Both CDF and DØ experiments report their final results on the CP asymmetry in the $B_s^0 \to J/\psi\phi$ decay with the full statistics. The CDF collaboration reconstructs [105] about 11000 such decays using the integrated luminosity 9.6 fb^{-1}. The result of this analysis is presented in Fig. 25 as the confidence regions in $\phi^{J/\psi\phi} - \Delta\Gamma_s$ plane. It can be seen that the obtained confidence region is consistent with the SM prediction within 1σ. The obtained confidence regions for the quantity $\beta_s^{J/\psi\phi} \equiv -\phi_s^{J/\psi\phi}/2$ is

$$\begin{aligned} \beta_s^{J/\psi\phi} &\in [-\pi/2, -1.51] \cup [-0.06, 0.30] \cup [1.26, \pi/2] \text{ at } 68\% \text{ C.L.} \\ \beta_s^{J/\psi\phi} &\in [-\pi/2, -1.36] \cup [-0.21, 0.53] \cup [1.04, \pi/2] \text{ at } 95\% \text{ C.L.} \end{aligned} \tag{66}$$

A similar analysis of $B_s^0 \to J/\psi\phi$ decay by the DØ collaboration [106] is based on 6500 signal events collected using the integrated luminosity 8 fb^{-1}. The result of this analysis is shown in Fig. 25. The obtained confidence region is consistent with the SM prediction, and the p-value for the SM point is 29.8%. The following values are obtained in this analysis:

$$\begin{aligned} \tau_s &= 1.443^{+0.038}_{-0.035} \text{ ps}, \\ \Delta\Gamma_s &= 0.163^{+0.065}_{-0.064} \text{ ps}^{-1}, \\ \phi_s^{J/\psi\phi} &= -0.55^{+0.38}_{-0.36}. \end{aligned} \tag{67}$$

Both results are consistent with each other and with the SM prediction. The latest result from the LHC experiments ATLAS [107] and LHCb[108] agrees with the values obtained at the Tevatron. The precision of the LHCb measurement is

particularly good, since it is an experiment dedicated to the B physics studies. Using a data sample of 0.37 fb^{-1}, they obtained

$$\Gamma_s = [0.657 \pm 0.009\ (\text{stat}) \pm 0.008\ (\text{syst})]\ \text{ps}^{-1}, \quad (68)$$

$$\Delta\Gamma_s = [0.123 \pm 0.029\ (\text{stat}) \pm 0.011\ (\text{syst})]\ \text{ps}^{-1}, \quad (69)$$

$$\phi_s^{J/\psi\phi} = 0.15 \pm 0.18\ (\text{stat}) \pm 0.06\ (\text{syst}). \quad (70)$$

The combination of all results on the CP violation in the $B_s^0 \to J/\psi\phi$ decay is performed by the Heavy Flavour Averaging Group (HFAG) [81]. The corresponding plot is shown in Fig. 25. The agreement of all measurements in this channel is reasonably good. It is one of the excellent examples of continuity of the B physics program from Tevatron to LHC. An excellent agrement of all results with the SM prediction reduces the prospects of detecting the new physics contribution in this channel.

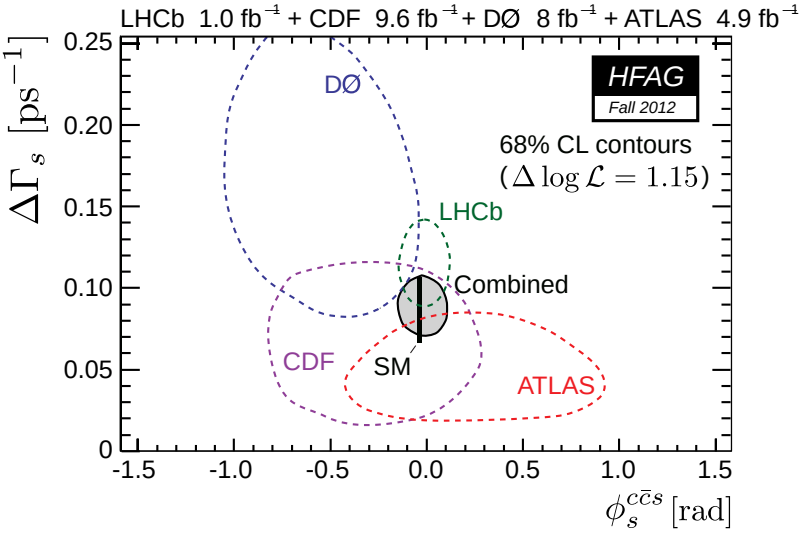

Figure 25: Constraints of all measurements of CP violation in $B_s^0 \to J/\psi\phi$ in the $\phi_s^{J/\psi\phi}$–$\Delta\Gamma_s$ plane taken from Ref. [81].

7.2 CP asymmetry in mixing of neutral B mesons

Studies of the CP asymmetry in mixing of neutral B_q^0 ($q = d, s$) mesons provide another possibility to search for the deviations from the SM prediction. This type of asymmetry is described by the CP violating phase ϕ_q, which is defined

as

$$\phi_q \equiv \arg\left(-\frac{m_q^{12}}{\Gamma_q^{12}}\right). \tag{71}$$

The parameters m_q^{12} and Γ_q^{12} are the complex non-diagonal elements of the mass mixing matrix. They are related to the observable quantities Δm_q and $\Delta\Gamma_q$ as

$$\Delta M_q = 2\left|m_q^{12}\right|, \qquad \Delta\Gamma_q = 2\left|\Gamma_q^{12}\right|\cos\phi_q. \tag{72}$$

The CP violating phase ϕ_q can be extracted from the charge asymmetry $a_{\rm sl}^q$ for "wrong-charge" semileptonic B_q^0-meson decay induced by oscillations, which is defined as

$$a_{\rm sl}^q = \frac{\Gamma(\bar{B}_q^0(t)\to l^+X) - \Gamma(B_q^0(t)\to l^-X)}{\Gamma(\bar{B}_q^0(t)\to l^+X) + \Gamma(B_q^0(t)\to l^-X)}. \tag{73}$$

This quantity is independent of the decay time t, and can be expressed as

$$a_{\rm sl}^q = \frac{\left|\Gamma_q^{12}\right|}{\left|M_q^{12}\right|}\sin\phi_q = \frac{\Delta\Gamma_q}{\Delta M_q}\tan\phi_q. \tag{74}$$

The SM predicts the values of $a_{\rm sl}^d$ and $a_{\rm sl}^s$ which are not detectable with the current experimental precision [104]:

$$a_{\rm sl}^d|_{\rm SM} = -(4.1\pm0.6)\times10^{-4}, \quad a_{\rm sl}^s|_{\rm SM} = (1.9\pm0.3)\times10^{-5}. \tag{75}$$

Additional contributions to CP violation via loop diagrams appear in some extensions of the SM [109, 110, 111, 112, 113, 114, 115, 116] and can result in these asymmetries within experimental reach.

In experimental measurements the muon is much easier to identify than any other lepton, therefore all experimental results on the semileptonic charge asymmetry are obtained with $l = \mu$ in Eq. (73). The DØ experiment performed several measurements of the semileptonic B^0 and B_s^0 charge asymmetry. The polarities of the toroidal and solenoidal magnetic fields of DØ detector were regularly reversed so that the four solenoid-toroid polarity combinations were exposed to approximately the same integrated luminosity. This feature is especially important in the measurements of the charge asymmetry, because the reversal of magnets polarities allows for a cancellation of first order effects related with the instrumental asymmetry and the reduction of the corresponding systematic uncertainty.

One of DØ results[117, 118] consists in measuring the like-sign dimuon charge asymmetry $A_{\rm sl}^b$. This quantity is defined as

$$A_{\rm sl}^b \equiv \frac{N_b^{++} - N_b^{--}}{N_b^{++} + N_b^{--}}. \tag{76}$$

Here N_b^{++} and N_b^{--} represent the number of events containing two b hadrons decaying semileptonically and producing two positive or two negative muons,

respectively. Assuming that this asymmetry is produced by CP violation in the mixing of B^0 and B_s^0 mesons, it can be expressed as

$$A_{\rm sl}^b = C_d a_{\rm sl}^d + C_s a_{\rm sl}^s, \tag{77}$$

where the coefficients C_d and C_s depend on the mean mixing probabilities χ_d and χ_s and the production rates of B^0 and B_s^0 mesons. Using the integrated luminosity of 9.1 fb^{-1}, the DØ experiment obtained

$$A_{\rm sl}^b = (-0.787 \pm 0.172({\rm stat}) \pm 0.093({\rm syst}))\%. \tag{78}$$

This result differs by 3.9 standard deviation from the SM prediction. From the study of the impact parameter dependence of the asymmetry, the DØ experiment extracted the separate values of $a_{\rm sl}^d$ and $a_{\rm sl}^s$

$$\begin{aligned} a_{\rm sl}^d &= (-0.12 \pm 0.52)\%, \\ a_{\rm sl}^s &= (-1.81 \pm 1.06)\%. \end{aligned} \tag{79}$$

The correlation ρ_{ds} between these two quantities is

$$\rho_{ds} = -0.799. \tag{80}$$

The precision of these quantities is comparable with the available world average measurements.

The DØ experiment also performed separate measurements of the asymmetries $a_{\rm sl}^d$ and $a_{\rm sl}^s$ using the semileptonic decays $B^0 \to \mu^+ \nu D^- X$, $B^0 \to \mu^+ \mu D^{*-} X$,[119] and $B_s^0 \to \mu^+ \nu D_s^- X$ [120], respectively. They obtained the following values:

$$a_{\rm sl}^d = (+0.68 \pm 0.45({\rm stat}) \pm 0.14({\rm syst}))\%, \tag{81}$$

$$a_{\rm sl}^s = (-1.08 \pm 0.72({\rm stat}) \pm 0.17({\rm syst}))\%. \tag{82}$$

Left plot in Fig. 26, taken from Ref. [119], presents the combination of all results of the DØ experiment on the CP asymmetry in mixing of neutral B mesons, plotted in the $(a_{\rm sl}^d, a_{\rm sl}^s)$ plane. It can be seen that the independent DØ measurements agree well between each other. The combined values of $a_{\rm sl}^d$ and $a_{\rm sl}^s$ asymmetries, including the measurement of $a_{\rm sl}^d$ asymmetry from B factories [81], is

$$\begin{aligned} a_{\rm sl}^d &= (0.07 \pm 0.27)\%, \\ a_{\rm sl}^s &= (-1.67 \pm 0.54)\%. \end{aligned} \tag{83}$$

The correlation ρ_{ds} between these two quantities is

$$\rho_{ds} = -0.46. \tag{84}$$

The p-value of the combination with respect to the SM point is 0.0037, corresponding to an inconsistency at the 2.9 standard deviation level.

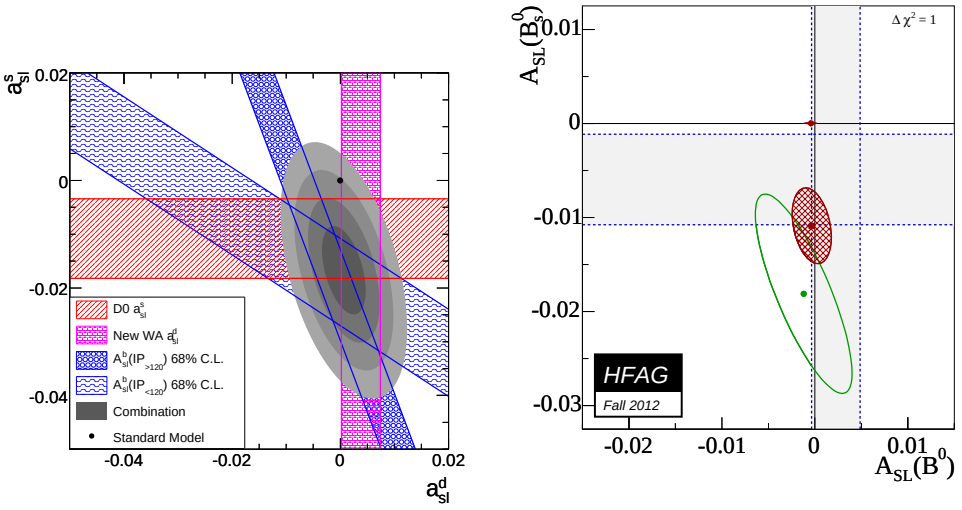

Figure 26: Left plot taken from Ref. [119]: Combination of measurements of $a^d_{\rm sl}$ (D0 [119] and existing world-average from B factories [14]), $a^s_{\rm sl}$ (D0 [120]), and the two impact-parameter-binned constraints from the same-charge dimuon asymmetry $A^b_{\rm sl}$ (D0 [117]). The bands represent the ± 1 standard deviation uncertainties on each measurement. The ellipses represent the 1, 2, 3, and 4 standard deviation two-dimensional confidence level regions of the combination. Right plot: Combination of all measurements of $a^d_{\rm sl}$ and $a^s_{\rm sl}$ taken from Ref. [81]. the vertical band is the average of the pure B^0 measurements performed at CLEO, BABAR, Belle and D0, the horizontal band is the average of the pure B^0_s measurements performed at D0 and LHCb with semileptonic Bs decays, the green ellipse is the D0 measurement with same-sign dileptons, and the read ellipse is the result of the two-dimensional averaging. The red point close to (0,0) is the SM prediction [104] with errors bars multiplied by 10.

Recently, the LHCb collaboration performed a similar measurement[121] of the asymmetry $a^s_{\rm sl}$ using the decays $B^0_s \to \mu^+\nu D^-_s X$. They obtained

$$a^s_{\rm sl} = (-0.24 \pm 0.54({\rm stat}) \pm 0.33({\rm syst}))\%. \quad (85)$$

All these results are consistent within 2 standard deviations, although the LHCb measurement does not confirm the significant deviation from the SM observed by the DØ experiment. The combination of all available results on $a^d_{\rm sl}$ and $a^s_{\rm sl}$ is performed by HFAG and is given in Ref. [81]. The obtained result is

$$\begin{aligned} a^d_{\rm sl} &= (0.03 \pm 0.21)\%, \\ a^s_{\rm sl} &= (-1.09 \pm 0.40)\%. \end{aligned} \quad (86)$$

It deviates from the SM prediction by 2.4 standard deviations. Right plot in Fig. 26 presents the result of this combination.

7.3 Other studies of CP asymmetry

The CDF collaboration performed an extensive study[122] of CP asymmetry in the two-body decays of B hadrons to light hadrons. They used 9.3 fb^{-1} of available statistics. In particular, they studied the direct CP violation in $B^0_s \to K^-\pi^+$ decay. This decay have been proposed as a clean test for the new physics contribution [123, 124]. The SM predicts an asymmetry $\sim 30\%$ in this decay. Any discrepancy from this prediction may indicate the contribution from non-SM amplitudes.

Since the particle identification capabilities of the CDF detector are limited, the main task is to disentangle the contribution of different decays in the invariant mass distribution. Figure 27 shows the result of these efforts. All hadrons are assigned the pion mass, and the observed $\pi^+\pi^-$ invariant mass distribution is presented as the superposition of different two-body decays of B hadrons. The invariant mass distribution of individual channels is obtained from the simulation. An unbinned likelihood fit, incorporating kinematic and particle identication information is used to determine the fraction of each individual mode. As a result of this study, the following values of CP asymmetry in different decay modes were obtained:

$$\frac{{\rm Br}(\bar{B}^0_d \to K^-\pi^+) - {\rm Br}(B^0 \to K^+\pi^-)}{{\rm Br}(\bar{B}^0_d \to K^-\pi^+) + {\rm Br}(B^0 \to K^+\pi^-)} = -0.083 \pm 0.013({\rm stat}) \pm 0.003({\rm syst}), \quad (87)$$

$$\frac{{\rm Br}(\bar{B}^0_s \to K^+\pi^-) - {\rm Br}(B^0 \to K^-\pi^+)}{{\rm Br}(\bar{B}^0_s \to K^+\pi^-) + {\rm Br}(B^0_s \to K^-\pi^+)} = +0.22 \pm 0.07({\rm stat}) \pm 0.02({\rm syst}), \quad (88)$$

$$\frac{{\rm Br}(\Lambda^0_b \to p\pi^-) - {\rm Br}(\bar{\Lambda}^0_b \to \bar{p}\pi^+)}{{\rm Br}(\Lambda^0_b \to p\pi^-) + {\rm Br}(\bar{\Lambda}^0_b \to \bar{p}\pi^+)} = +0.07 \pm 0.07({\rm stat}) \pm 0.03({\rm syst}), \quad (89)$$

$$\frac{{\rm Br}(\Lambda^0_b \to pK^-) - {\rm Br}(\bar{\Lambda}^0_b \to \bar{p}K^+)}{{\rm Br}(\Lambda^0_b \to PK^-) + {\rm Br}(\bar{\Lambda}^0_b \to \bar{p}K+)} = -0.09 \pm 0.08({\rm stat}) \pm 0.04({\rm syst}). \quad (90)$$

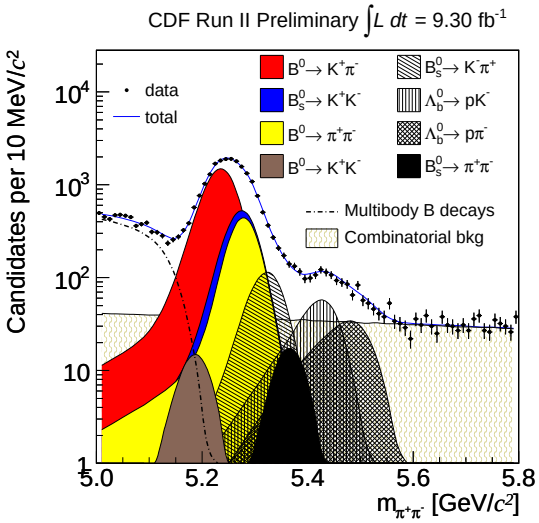

Figure 27: Mass distribution of reconstructed candidates, $m(\pi\pi)$ taken from Ref. [122]. The charged pion mass is assigned to both particles. The total projection is overlaid on the data distribution.

The DØ collaboration performed a measurement[126] of the charge asymmetry in the $B^+ \to J/\psi K^+(\pi^+)$ decay using 2.8 fb^{-1} of available statistics. This asymmetry is defined as

$$A_{CP} = \frac{\mathrm{Br}(B^- \to J/\psi K^-(\pi^-) - \mathrm{Br}(B^+ \to J/\psi K^+(\pi^+))}{\mathrm{Br}(B^- \to J/\psi K^-(\pi^-) - \mathrm{Br}(B^+ \to J/\psi K^+(\pi^+))}. \quad (91)$$

A non-zero value of $A_{CP}(B^+ \to J/\psi K^+(\pi^+))$ corresponds to direct CP violation in this decay. The SM predicts[125] a small $A_{CP}(B^+ \to J/\psi K^+ \sim 0.003$. Therefore, the observation of this asymmetry at a higher level would be very interesting. The results obtained with more than 40000 $B^+ \to J/\psi K^+(\pi^+)$ decays are:

$$A_{CP}(B^+ \to J/\psi K^+) = +0.0075 \pm 0.0061(\mathrm{stat}) \pm 0.0027(\mathrm{syst})), \quad (92)$$

$$A_{CP}(B^+ \to J/\psi \pi^+) = -0.09 \pm 0.08(\mathrm{stat}) \pm 0.03(\mathrm{syst})). \quad (93)$$

$$(94)$$

7.4 Summary of the CP asymmetry studies

In conclusion, an extensive search for the new sources of CP asymmetry is performed at the Tevatron. Many unique and world best results on the CP asymmetry in the B_s^0 decays are obtained. However, no clear indication of the deviation of the CP asymmetry phenomena from the SM prediction is observed. These studies are continued by the LHC experiment and the new level of precision in these studies is expected to be achieved.

8 Conclusions

A decade of intensive study of B hadrons at the Tevatron produced an impressive list of fascinating results. Among the milestones achieved at the Tevatron, we can mention the discovery of many B hadrons and the precise measurement of their properties, including the mass and lifetime of B_s^0 meson and Λ_b^0 baryon. The measurement of the oscillation frequency of B_s^0 meson provides a crucial constraint on the unitarity of the CKM matrix. The search for rare decay $B_s^0 \to \mu^+\mu^-$, although not attaining the expected SM level, nevertheless imposes an important constraint on the possible extensions of the SM. Many studies of the CP violation in the decays and mixing of the B_s^0 meson are unique or world best. There is an indication of a possible deviation from the SM prediction in the CP asymmetry in mixing of B_s^0 meson. It requires a verification by the independent measurements at LHC, but regardless the outcome of this cross check, the research pioneered at the Tevatron gives a strong boost to further studies in this direction. The list of important results may be extended to many other excellent measurements performed at the Tevatron. Regrettably, due to a luck of space, some of them are omitted from this review. But probably the most important achievement of the Tevatron experiments is a clear and indubitable demonstration of a possibility and high value of performing B physics at hadron

collider, which provides an important support for extending this program at the LHC.

Acknowledgements

All results presented in this review are obtained by the common efforts of many people of the CDF and DØ collaboration, and I want to expresses my gratitude to all my colleagues from both experiments. Without their relentless work neither of these result was possible. I also want to thank the scientists of the accelerating division of the Fermilab laboratory, who provided a stable work of the Tevatron collider, breaking many records of performance, which was crucial for obtaining all results presented here.

References

[1] CDF Collab. (A. Abulencia *et al.*), *J. Phys. G* **34**, 2457 (2007).

[2] A. Sill *et al.*, *Nucl. Instrum. Methods in Phys. Res. A* **447**, 1 (2000).

[3] CDF Collab. (A. Affolder *et al.*), *Nucl. Instrum. Methods in Phys. Res. A* **526**, 249 (2004).

[4] C. S. Hill (on behalf of the CDF Collaboration), *Nucl. Instrum. Methods in Phys. Res. A* **530**, 1 (2004).

[5] G. Ascoli *et al.*, *Nucl. Instrum. Methods in Phys. Res. A* **268**, 33 (1988).

[6] T. Dorigo *et al.*, *Nucl. Instrum. Methods in Phys. Res. A* **461**, 560 (2001).

[7] E. J. Thomson *et al.*, *IEEE Trans. Nucl. Sci.* **49**, 1063 (2002).

[8] CDF Collab. (J. A. Adelman *et al.*), *Nucl. Instrum. Methods in Phys. Res. A* **572**, 361 (2007).

[9] CDF Collab. (A. Abulencia *et al.*)), *Phys. Rev. Lett.* **98**, 122002 (2007).

[10] D0 Collab. (V.M. Abazov *et al.*), *Nucl. Instrum. Methods in Phys. Res. A* **565**, 463 (2006).

[11] V.M. Abazov *et al.*, *Nucl. Instrum. Methods in Phys. Res. A* **552**, 372 (2005).

[12] S.N. Ahmed *et al.*, Nucl. Instrum. Methods in Phys. Res. A **634**, 8 (2011);

[13] R. Angstadt *et al.*, Nucl. Instrum. Methods in Phys. Res. A **622**, 298 (2010).

[14] J. Beringer et al. (Particle Data Group), *Phys. Rev. D* **86**, 010001 (2012) (URL: http://pdg.lbl.gov)

[15] CDF Collab. (D. Acosta *et al.*), *Phys. Rev. Lett.* **96**, 202001 (2006).

[16] CLEO Collab. (S.E. Csorna *et al.*), *Phys. Rev. D* **61**, 111101 (2000).

[17] LHCb Collab. (R. Aaij *et al.*), *Phys. Lett. B* **708**, 241 (2012).

[18] N. Brambilla *et al.*, arXiv:hep-ph/0412158.

[19] E. J. Eichten and C. Quigg, *Phys. Rev. D* **49**, 5845 (1994);

[20] W. K. Kwong and J. L. Rosner, *Phys. Rev. D* **44**, 212 (1991);

[21] S. Godfrey, *Phys. Rev. D* **70**, 054017 (2004).

[22] I. F. Allison *et al.*, *Phys. Rev. Lett.* **94**, 172001 (2005).

[23] CDF Collab. (T. Aaltonen *et al.*), *Phys. Rev. Lett.* **100**, 182002 (2008).

[24] D0 Collab. (V. Abazov *et al.*), *Phys. Rev. Lett.* **101**, 012001 (2008).

[25] LHCb Collab. (R. Aaij *et al.*), arXiv:1209.5634 [hep-ex].

[26] For a review see A. V. Manohar and M. B. Wise, *Camb. Monogr. Part. Phys. Nucl. Phys. Cosmol.* **10** (2000) 1, and references therein.

[27] CDF Collab. (T. Aaltonen *et al.*), *Phys. Rev. D* **85**, 092011 (2012).

[28] E. Jenkins, *Phys. Rev D* **54**, 4515 (1996); **55**, R10 (1997);

[29] N. Mathur, R. Lewis and R. M. Woloshyn, *Phys. Rev. D* **66**, 014502 (2002);

[30] R. Lewis and R. M. Woloshyn, *Phys. Rev. D* **79**, 014502 (2009).

[31] D. Ebert, R. N. Faustov and V. O. Galkin, *Phys. Rev. D* **72**, 034026 (2005);

[32] D. Ebert, R. N. Faustov, and V. O. Galkin, *Phys. Lett. B* **659**, 612 (2008);

[33] D. Ebert, R. N. Faustov, and V. O. Galkin, *Phys. Atom. Nucl.* **72**, 178 (2009).

[34] M. Karliner, B. Keren-Zur, H. J. Lipkin, and J. L. Rosner, *Annals Phys.* **324**, 2 (2009).

[35] J. L. Rosner, *Phys. Rev. D* **75**, 013009 (2007).

[36] CDF Collab. (T. Aaltonen *et al.*), *Phys. Rev. Lett.* **99**, 202001 (2007).

[37] D0 Collab. (V. Abazov *et al.*), *Phys. Rev. Lett.* **99**, 052001 (2007).

[38] CDF Collab. (T. Aaltonen *et al.*), *Phys. Rev. Lett.* **99**, 052002 (2007).

[39] CDF Collab. (T. Aaltonen *et al.*), *Phys. Rev. D* **80**, 072003 (2009).

[40] CDF Collab. (T. Aaltonen *et al.*), *Phys. Rev. Lett.* **107**, 102001 (2011).

[41] D0 Collab. (V. Abazov *et al.*), *Phys. Rev. Lett.* **101**, 232002 (2008).

[42] T. Matsuki and T. Morii, *Phys. Rev. D* **56**, 5646 (1997);

[43] T. Matsuki, T. Morii and K. Sudoh, *Progr. Theor. Phys.* **117**, 1077 (2007).

[44] M. Di Pierro and E. Eichten, *Phys. Rev. D* **64**, 114004 (2001).

[45] E.J. Eichten, C.T. Hill, C. Quigg, *Phys. Rev. Lett.* **71**, 4116 (1993).

[46] N. Isgur, Phys. Rev. D **57**, 4041 (1998);

[47] N. Isgur and M. B. Wise, *Phys. Lett. B* **232**, 113 (1989);

[48] N. Isgur and M. B. Wise, *Phys. Lett. B* **237**, 527 (1990).

[49] D. Ebert, V.O. Galkin, and R.N. Faustov, *Phys. Rev. D* **57**, 5663 (1998), Erratum *Phys. Rev. D* **59**, 019902 (1999).

[50] A.H. Orsland, H. Hogaasen, *Eur. Phys. J. C* **9**, 503 (1999).

[51] A. Falk, T. Mehen, *Phys. Rev. D* **53**, 231 (1996).

[52] D0 Collab. (V. Abazov *et al.*), *Phys. Rev. Lett.* **99**, 172001 (2007).

[53] CDF Collab. (T. Aaltonen *et al.*), *Phys. Rev. Lett.* **102**, 102003 (2009).

[54] CDF Collab. (T. Aaltonen *et al.*), *Phys. Rev. Lett.* **100**, 082001 (2008).

[55] D0 Collab. (V. Abazov *et al.*), *Phys. Rev. Lett.* **100**, 082002 (2008).

[56] W.-M. Yao et al. (Particle Data Group), *J. Phys. G* **33**, 1 (2006).

[57] CDF Collab. (T. Aaltonen *et al.*), *Phys. Rev. Lett.* **106**, 121804 (2011).

[58] Belle Collab. (K. Abe *et al.*), *Phys. Rev. D* **71**, 072003 (2005). Erratum-ibid. **71**, 079903 (2005).

[59] M. Beneke et al., *Nucl. Phys. B* **639**, 389 (2002);

[60] E. Franco, V. Lubicz, F. Mescia, and C. Tarantino, *Nucl. Phys. B 633*, 212 (2002);

[61] C. Tarantino, *Eur. Phys. J. C* **33**, S895 (2004);

[62] A. J. Lenz, *AIP Conf. Proc.* **1026**, 36 (2008).

[63] I. Bigi et al., in *B Decays*, 2nd ed., S. Stone (ed.), World Scientific, Singapore (1994).

[64] F. Gabbiani, A. Onischenko, and A. Petrov, *Phys. Rev. D* **68**, 114006 (2003)

[65] F. Gabbiani, A. Onischenko, and A. Petrov, *Phys. Rev. D* **70**, 094031 (2004).

[66] D0 Collab. (V. Abazov *et al.*), *Phys. Rev. Lett.* **94**, 182001 (2005).

[67] D0 Collab. (V. Abazov *et al.*), *Phys. Rev. Lett.* **97**, 241801 (2006).

[68] CDF Collab. (T. Aaltonen *et al.*), *Phys. Rev. Lett.* **107**, 272001 (2011).

[69] CDF Collab. (T. Aaltonen *et al.*), *Phys. Rev. D* **84**, 052012 (2011).

[70] M. Beneke and G. Buchalla, *Phys. Rev. D* **53**, 4991 (1996).

[71] V. V. Kiselev, A. E. Kovalsky and A. K. Likhoded, *Nucl. Phys. B* **585**, 353 (2000).

[72] V. Kiselev, arXiv:hep-ph/0308214 (2003), and references therein.

[73] C.-H. Chang, S.-L. Chen, T.-F. Feng, and X.-Q. Li, *Phys. Rev. D* **64**, 014003 (2001).

[74] CDF Collab. (T. Aaltonen *et al.*), CDF note 9294, (2008) http://www-cdf.fnal.gov/physics/new/bottom/080327.blessed-BC_LT_SemiLeptonic/.

[75] CDF Collab. (T. Aaltonen *et al.*), arXiv:1210.2366 [hep-ex].

[76] D0 Collab. (V. Abazov *et al.*), *Phys. Rev. Lett.* **102**, 092001 (2009).

[77] C. Tarantino, *Eur. Phys. J. C* **33**, s895 (2004).

[78] D0 Collab. (V. Abazov *et al.*), *Phys. Rev. Lett.* **99**, 182001 (2007).

[79] D0 Collab. (V. Abazov *et al.*), *Phys. Rev. D* **85**, 112003 (2012).

[80] CDF Collab. (T. Aaltonen *et al.*), *Phys. Rev. Lett.* **104**, 102002 (2010).

[81] Heavy Flavour Averaging group (Y. Amhis *et al.*), arXiv:1207.1158 [hep-ex] and online update at http://www.slac.stanford.edu/xorg/hfag

[82] CKMfitter group (J. Charles *et al.*), *Eur. Phys. J. C* **41**, 1 (2005), A. Höocker *et al.*, *Eur. Phys. J. C* **21**, 225 (2001), see also updates at http://ckmfitter.in2p3.fr/.

[83] UTfit Collab. (M. Bona *et al.*), *J. High Energy Phys.* **507**, 28 (2005), and updates at http://www.utfit.org/;

[84] UTfit Collab. (M. Bona *et al.*), *J. High Energy Phys.* **0803**, 28 (2008).

[85] D0 Collab. (V. Abazov *et al.*), *Phys. Rev. Lett.* **97**, 021802 (2006).

[86] D0 Collab. (V. Abazov *et al.*), *Phys. Rev. D* **74**, 112002 (2006).

[87] CDF Collab. (T. Abulencia *et al.*), *Phys. Rev. Lett.* **97**, 242003 (2006).

[88] HPQCD Collab. (E. Gamiz *et al.*), *Phys. Rev. D* **80**, 014503 (2009).

[89] A. J. Buras *et al.*, *Eur. Phys. J. C* **72**, 2172 (2012).

[90] A. J. Buras *et al.*, *J. High Energy Phys.* **10**, 009 (2010).

[91] C. Hamzaoui, M. Pospelov, and M. Toharia, *Phys. Rev. D* **59**, 095005 (1999).

[92] S. R. Choudhury and N. Gaur, *Phys. Lett. B* **451**, 86 (1999);

[93] K.S. Babu and C. Kolda, *Phys. Rev. Lett.* **84**, 228 (2000).

[94] A. Buras and J. Girrbach, *Acta Physica Polonica B* **43**, 1427 (2012) and arXiv: 1204.5604 [hep-ph] (2012), and references therein.

[95] D0 Collab. (V. Abazov *et al.*), *Phys. Lett. B* **693**, 539 (2010).

[96] CDF Collab. (T. Aaltonen *et al.*), *Phys. Rev. Lett.* **107**, 191801 (2011).

[97] CDF Collab. http://www-cdf.fnal.gov/physics/new/bottom/120209.blessed-bmumu10fb/

[98] LHCb Collab. (R. Aaij *et al.*), arXiv:1211.2674 [hep-ex].

[99] CDF Collab. http://www-cdf.fnal.gov/physics/new/bottom/120628.blessed-b2smumu_96/

[100] R. Aleksan *et al.*, *Phys. Lett. B* **316**, 567 (1993).

[101] D0 Collab. (V. Abazov *et al.*), *Phys. Rev. Lett.* **99**, 241801 (2010).

[102] CDF Collab. (T. Aaltonen *et al.*), *Phys. Rev. Lett.* **108**, 201801 (2012).

[103] P. Huet and E. Sather, *Phys. Rev. D* **51**, 379 (1995).

[104] A. Lenz and U. Nierste, arXiv:1102.4274 (2011).

[105] CDF Collab. (T. Aaltonen *et al.*), *Phys. Rev. Lett.* **109**, 171802 (2012).

[106] D0 Collab. (V.M. Abazov *et al.*), *Phys. Rev. D* **85**, 032006 (2012).

[107] ATLAS Collab. (G. Aad *et al.*), arXiv: 1208.0572 [hep-ex] (2012).

[108] LHCb Collab. (R. Aaij *et al.*), *Phys. Rev. Lett.* **108**, 101803 (2012).

[109] L. Randall and S. Su, *Nucl. Phys. B* **540**, 37 (1999).

[110] J.L. Hewett, arXiv:hep-ph/9803370 (1998).

[111] G.W.S. Hou, arXiv:0810.3396 [hep-ph] (2008).

[112] A. Soni *et al.*, *Phys. Lett. B* **683**, 302 (2010);

[113] A. Soni *et al.*, *Phys. Rev. D* **82**, 033009 (2010) and references therein.

[114] M. Blanke *et al.*, J. High Energy Phys. **12**, 003 (2006);

[115] W. Altmannshofer, *et al.*, Nucl. Phys. B **830**, 17 (2010).

[116] A. Buras and J. Girrbach, *Acta Physica Polonica B* **43**, 1427 (2012) and arXiv: 1204.5604 [hep-ph] (2012).

[117] D0 Collab. (V.M. Abazov *et al.*), *Phys. Rev. D* **82**, 032001 (2010).

[118] D0 Collab. (V.M. Abazov *et al.*), *Phys. Rev. D* **84**, 052007 (2011).

[119] D0 Collab. (V. Abazov *et al.*), *Phys. Rev. D* **86**, 072009 (2012).

[120] D0 Collab. (V. Abazov *et al.*), arXiv:1207.1769 [hep-ex] (2012).

[121] LHCb collaboration, Conference report LHCb-CONF-2012-022 (2012).

[122] CDF Collab., CDF note 10726, (2008)
http://www-cdf.fnal.gov/physics/new/bottom/120628.blessed-Bhh9fb/.

[123] M. Gronau and J. L. Rosner, *Phys. Lett. B* **482**, 71 (2000).

[124] H. J. Lipkin, *Phys. Lett. B* **621**, 126 (2005).

[125] W.-S. Hou, M. Nagashima and A. Soddu, arXiv:hep-ph/0605080 (2006).

[126] D0 Collab. (V. Abazov *et al.*), *Phys. Rev. Lett.* **100**, 211802 (2008).